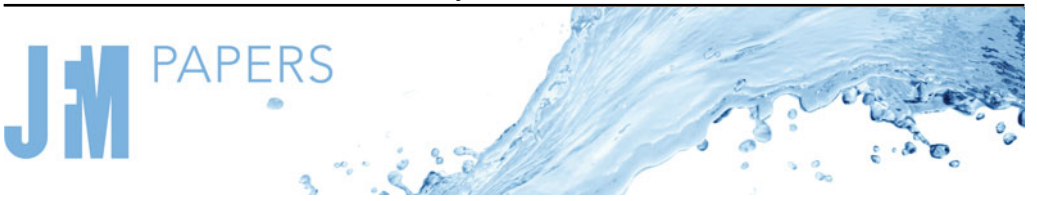
J. Fluid Mech. (2026), *vol.* 1029, A2, doi:10.1017/jfm.2026.11138



Three-layer water flows: Dirichlet–Neumann operators and approximations

Rossen I. Ivanov[1] **and Calin I. Martin**[2]

[1]School of Mathematics and Statistics, Technological University Dublin, City Campus, Grangegorman Lower, Dublin D07 ADY7, Ireland

[2]Faculty of Mathematics and Computer Science, Babes-Bolyai University, Mihail Kogalniceanu, Str. 1, Cluj-Napoca, Romania

Corresponding author: Calin I. Martin, calin.martin@ubbcluj.ro

(Received 9 April 2024; revised 31 July 2025; accepted 8 January 2026)

The object of investigation in this paper is the nonlinear equations of motion for two-dimensional inviscid water flows with piecewise constant density stratification in a three-layer fluid with a flat bottom, a free surface and two interfaces. We establish a Hamiltonian formulation for the nonlinear governing equations in this set-up. The Hamiltonian of the system and the equations of motion of the surface and of the interfaces are expressed with the help of the Dirichlet–Neumann (DN) operators, which are introduced for each of the layers. Then the linear equations for small amplitudes of the elevation of the surface and of the interfaces in the leading order are derived, from which a bi-cubic equation for the dispersion relation is obtained, whose solutions are analysed. The six real solutions for the possible propagation speeds (three positive, related to right-moving waves, and three negative, related to left-moving waves) have magnitudes of different order. Upper and lower bounds for the previously mentioned roots are also given in terms of the coefficients of the equation. Subsequently, approximate formulas for the propagation speeds are derived. The importance of the DN operators is further illustrated in a separate analysis of the three-layer model with flat surface (rigid lid). The full nonlinear evolution equations are expressed again in terms of the DN operators, and the equations in the linear regime and the weakly nonlinear propagation regime (the Boussinesq approximation) are derived by a proper expansion of the DN operators. Limits to the two-layer free surface model are obtained as well. The obtained results are applicable to internal waves in lakes and in the ocean as well as to laboratory experiments with three superimposed fluid layers.

Key words: stratified flows, Hamiltonian theory, waves/free-surface flows

© The Author(s), 2026. Published by Cambridge University Press.

https://doi.org/10.1017/jfm.2026.11138 Published online by Cambridge University Press

1. Introduction

Flow stratification – assumed to be of piecewise constant type in our work – is an intrinsic characteristic of geophysical water flows, particularly relevant to large-scale oceanic movements (cf. Gill 1982; Marshall & Plumb 2016; Constantin & Johnson 2017; Vallis 2017). Strongly influenced by variations in temperature and salinity, density fluctuations occur frequently in the ocean and lead to a layered structure: fluid parcels of differing densities arrange themselves such that denser layers lie beneath lighter ones (cf. Kessler & McPhaden 1995; Fedorov & Brown 2009; Cushman-Roisin & Beckers 2011; Constantin & Johnson 2015). This vertical stratification results in the formation of interfaces between layers of distinct densities. Such a pronounced density stratification occurs within a region approximately 150 km wide on each side of the Equator, extending longitudinally over approximately 16 000 km in the Pacific Ocean. This stratification gives rise to a sharp thermocline (also referred to as a pycnocline), which acts as a waveguide for internal waves; cf. Fedorov & Brown (2009) and Constantin & Johnson (2015). At times, internal waves might have appreciable amplitudes: field data provide evidence for tide-generated internal waves with amplitudes in excess of 100 m, extending over 100 km; cf. Simmons *et al.* (2011). Detailed, exact solutions depicting density stratified geophysical flows exhibiting internal waves were presented by Constantin (2013, 2014).

From a practical side, the understanding of internal waves dynamics is important for mixing processes in oceans and submarine navigation, as well as for the need to quantify induced loads on submerged marine platforms.

Concerning the vertical stratification structure, it is widely accepted in oceanography (see Sutherland 2010) that the ocean is effectively subdivided into layers according to the strength of its stratification. Accordingly we have: adjacent to the surface lies the mixed layer, named for the wind-driven stirring of surface waters; beneath it is the the strongly stratified thermocline; and below that is the weakly stratified deep layer composed of cold, dense water that constitutes the bulk of the ocean's mass. Complementing this conceptual model, a series of laboratory experiments using a wind flume (Shintani & Umeyama 2001) simulated a three-layer density-stratified water body in which the middle layer (thermocline) was intentionally made thick, closely matching the thickness of the upper and lower layers. This deliberate configuration was designed to reflect stratification patterns observed in natural lakes, and to isolate the role of the thermocline. The study revealed that the thickness of the middle layer is a critical factor in shaping the system's response to wind forcing, significantly influencing internal wave dynamics, energy transfer, and vertical mixing across the stratified column.

Minding the previous aspects concerning the type of layering in physically reasonable ocean flows, we consider in this study three-layer stratified water flows: the fluid domain is bounded above by the free surface and below by the (rigid) bottom boundary, and is split in three layers of constant, but different density. This type of stratification significantly complicates the analysis of an already highly intricate nonlinear problem. To alleviate these difficulties, we will rewrite the governing equations by means of a Hamiltonian (re)formulation. Such a reformulation highlights structural properties and has the advantage that it also reduces the numbers of variables in a way that results in significant simplifications. Note that the Hamiltonian formulation of the governing equations for two-dimensional gravity water flows was pioneered in Zakharov (1968) for irrotational flows, and was extended to rotational flows with constant vorticity in Constantin, Ivanov & Prodanov (2007), Wahlén (2007, 2008) and Compelli & Ivanov (2017), and variable bottom in Craig *et al.* (2005), Compelli, Ivanov & Todorov (2018) and Compelli *et al.* (2019). The Hamiltonian formulation for two-dimensional irrotational

https://doi.org/10.1017/jfm.2026.11138 Published online by Cambridge University Press

two-layer gravity water flows with a free surface was developed in Craig, Guyenne & Kalisch (2005), and the rotational counterpart with constant vorticity and constant density in each layer was obtained in Constantin, Ivanov & Martin (2016) for the case of periodic flows. The validity of the Hamiltonian perspective in the presence of Coriolis forces in the equatorial f-plane approximation, for zonal flows representing localised perturbations of an underlying pure current background state, was established in Constantin & Ivanov (2019). We note that the power and relevance of Hamiltonian methods in the study of water flows is reinforced by the work of Craig, Guyenne & Sulem (2015), where a relevant extension to three-dimensional flows is presented. Additionally, a mix of Hamiltonian methods and techniques related to the Dirichlet–Neumann (DN) operators is instrumental in the derivation of coupled nonlinear equations relating the interfaces and the traces of the velocity potentials on them, in various propagation regimes; cf. e.g. Craig *et al.* (2005, 2011, 2015) and § 7.5 of this work.

The two- and three-layer dynamics have been studied actively, and various approximations have been employed, from Kakutani & Yamasaki (1978) and Ovsyannikov (1979) to the more recent Choi & Camassa (1996, 1999), Camassa *et al.* (2021), Cotter, Holm & Percival (2010), Grimshaw *et al.* (2014), Ostrovsky & Helfrich (2019), de Melo Viríssimo & Milewski (2019) and Bona, Lannes & Saut (2008). For recent results concerning exact solutions (in Lagrangian and Eulerian coordinates) describing water flows with stratification of discontinuous type, we refer the reader to Constantin (2013, 2014), Matioc (2012), Massel (2015), Escher *et al.* (2020) and Martin (2021).

Our aim is to present a Hamiltonian formulation and the full nonlinear equations of motion of two-dimensional stratified water flows consisting of three layers, each of which has constant density. We adopt a versatile framework for our investigations: the density in each layer can have any value, with the proviso that the stratification is of stable type. Moreover, the layers can have any thicknesses, without any constraints.

The paper is organised as follows. After introducing the model set-up and the governing equations in § 2, we show in § 3 that they can be rewritten as an infinite-dimensional Hamiltonian system. Furthermore, in § 3 we present the resulting full nonlinear equations of motion. They are expressed in terms of the so-called DN operators, which are introduced for the three-layer setting with a free surface. In § 4, the dispersion relation for the leading order of the wave amplitudes is derived for arbitrary wavelengths. Section 5 is devoted to the dispersion relation in the long-wave limit which is an intricate bi-cubic equation, whose solutions are all real numbers according to arguments presented in Benton (1954), Yih (1980) and Baines (1995). Exploiting a result by Prodanov (2022*a*,*b*), we give lower and upper bounds for these solutions. The limit to two layers is presented in § 6. Approximate solutions in certain regimes are also given. Section 7 is devoted to the three-layer rigid lid case. There again we present the full equations in terms of the DN operators, then by the expansion of the operators, we recover the dispersion relation of the system, and in addition we obtain the equations of the widely used nonlinear Boussinesq regime. Although the present study focuses on the three-layer model pertinent to oceanographic dynamics, we emphasise that the analytical framework and methodologies developed herein are broadly applicable to a wide range of scenarios involving interfacial internal waves across stratified fluid layers, extending well beyond the confines of saline ocean environments, and also to higher-order nonlinear approximations, if the quadratic ones are insufficient for the analysis.

https://doi.org/10.1017/jfm.2026.11138 Published online by Cambridge University Press

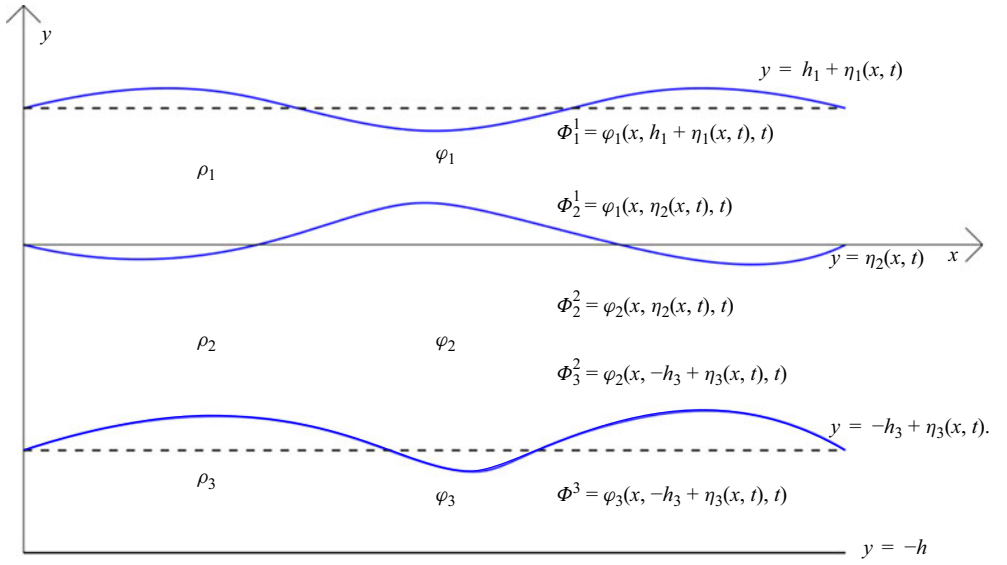


Figure 1. The system under study.

2. Model set-up and governing equations

We assume that the fluid domain consists of a union of layers Ω_i $(i = 1, 2, 3)$ depicted in figure 1 and defined as follows:

$$\begin{aligned}
\Omega_1 &:= \{(x, y, t) : x \in \mathbb{R}, t \in \mathbb{R}, \eta_2(x, t) < y < h_1 + \eta_1(x, t)\},\\
\Omega_2 &:= \{(x, y, t) : x \in \mathbb{R}, t \in \mathbb{R}, -h_3 + \eta_3(x, t) < y < \eta_2(x, t)\},\\
\Omega_3 &:= \{(x, y, t) : x \in \mathbb{R}, t \in \mathbb{R}, -h < y < -h_3 + \eta_3(x, t)\},
\end{aligned} \tag{2.1}$$

where h_1, h_3, h are positive constants such that $h > h_3$, and $\eta_i(x, t) \in \mathcal{S}(\mathbb{R})$ for $i = 1, 2, 3$ are Schwartz functions such that for all $i = 1, 2, 3$, the relations

$$\int_{\mathbb{R}} \eta_i(x, t)\, \mathrm{d}x = 0 \quad \text{for all} \quad t \tag{2.2}$$

hold. Relations (2.2) ensure that the average surface level of η_1 is at $y = h_1$, the average surface level of η_2 is at $y = 0$, and the average surface level of η_3 is at $y = -h_3$.

The density of the fluid is assumed to be piecewise constant at ρ_i $(i = 1, 2, 3)$ in the layer Ω_i for $i = 1, 2, 3$, and such that $\rho_1 < \rho_2 < \rho_3$ to account for the stable stratification. The same indicial notation will be used to denote the other physical quantities (e.g. the velocity field, the velocity potentials, the pressure). However, when we refer to the overall physical variable without specification of the layer, we will use the hat symbol placed on top of the variable. For example, $(\hat{u}, \hat{v})$ will denote the velocity field that takes the value (u_i, v_i) in the layer Ω_i, for $i = 1, 2, 3$. Using $\hat{P}$ to denote the pressure, the equations of motion for an incompressible, inviscid flow are Euler's equations

$$\begin{aligned}
\hat{u}_t + \hat{u}\hat{u}_x + \hat{v}\hat{u}_y &= -\frac{1}{\hat{\rho}}\hat{P}_x,\\
\hat{v}_t + \hat{u}\hat{v}_x + \hat{v}\hat{v}_y &= -\frac{1}{\hat{\rho}}\hat{P}_y - g
\end{aligned} \qquad \text{in} \quad \overline{\Omega_1 \cup \Omega_2 \cup \Omega_3}, \tag{2.3}$$

https://doi.org/10.1017/jfm.2026.11138 Published online by Cambridge University Press

and the equation of mass conservation

$$\hat{u}_x + \hat{u}_y = 0 \quad \text{in} \quad \overline{\Omega_1 \cup \Omega_2 \cup \Omega_3}. \tag{2.4}$$

Equations (2.3) and (2.4) are complemented by appropriate boundary conditions. At the free surface, the dynamic boundary condition

$$P_1 = P_{atm} \quad \text{on} \quad y = h_1 + \eta_1(x, t) \tag{2.5}$$

decouples the motion of the water from that of the air above, and at the same time ensures the balance of forces at the surface. Similarly, the balances of forces at the internal boundaries $y = \eta_2(x, t)$ and $y = -h_3 + \eta_3(x, t)$, respectively, are expressed by the conditions

$$P_1 = P_2 \quad \text{on} \quad y = \eta_2(x, t) \tag{2.6}$$

and

$$P_2 = P_3 \quad \text{on} \quad y = -h_3 + \eta_3(x, t). \tag{2.7}$$

The kinematic boundary conditions, which refer to the flat bed $y = -h$, the two interfaces $y = -h_3 + \eta_3(x, t)$ and $y = \eta_2(x, t)$, respectively, and to the free surface $y = h_1 + \eta_1(x, t)$, ensure that these surfaces are impermeable, thus no fluid particles cross them; they are stated as

$$\begin{aligned}
&v_1 = \eta_{1,t} + u_1\eta_{1,x} \quad \text{on} \quad y = h_1 + \eta_1(x, t),\\
&v_1 = \eta_{2,t} + u_1\eta_{2,x} \quad \text{and} \quad v_2 = \eta_{2,t} + u_2\eta_{2,x} \quad \text{on} \quad y = \eta_2(x, t),\\
&v_2 = \eta_{3,t} + u_2\eta_{3,x} \quad \text{and} \quad v_3 = \eta_{3,t} + u_3\eta_{3,x} \quad \text{on} \quad y = -h_3 + \eta_3(x, t),\\
&v_3 = 0 \quad \text{on} \quad y = -h.
\end{aligned} \tag{2.8}$$

Throughout the paper, we will assume that the fluid is rotation-free, i.e.

$$\hat{u}_y(x, y, t) - \hat{v}_x(x, y, t) = 0 \quad \text{for all} \quad (x, y, t) \in \overline{\Omega_1 \cup \Omega_2 \cup \Omega_3}. \tag{2.9}$$

The irrotationality assumption (2.9) allows us to introduce now in each layer Ω_i a velocity potential $\varphi_i \in C^1(\Omega_i)$ that satisfies

$$u_i = \varphi_{i,x} \quad \text{and} \quad v_i = \varphi_{i,y} \quad \text{for} \quad i = 1, 2, 3. \tag{2.10}$$

REMARK 2.1. *Note that due to (2.4), the velocity potentials* φ_i $(i = 1, 2, 3)$ *are harmonic functions in* Ω_i, $i = 1, 2, 3$.

We will use, in the course of the paper, the subscripts s_1, s_2, s_3 in order to denote evaluations of various quantities on the surfaces $y = h_1 + \eta_1(x, t)$, $y = \eta_2(x, t)$ and $y = -h_3 + \eta_3(x, t)$, respectively. The kinematic boundary conditions can now be written as

$$\eta_{1,t} = (\varphi_{1,y})_{s_1} - \eta_{1,x}(\varphi_{1,x})_{s_1}, \tag{2.11}$$

$$\eta_{2,t} = (\varphi_{1,y})_{s_2} - \eta_{2,x}(\varphi_{1,x})_{s_2} = (\varphi_{2,y})_{s_2} - \eta_{2,x}(\varphi_{2,x})_{s_2}, \tag{2.12}$$

$$\eta_{3,t} = (\varphi_{2,y})_{s_3} - \eta_{3,x}(\varphi_{2,x})_{s_3} = (\varphi_{3,y})_{s_3} - \eta_{3,x}(\varphi_{3,x})_{s_3}. \tag{2.13}$$

https://doi.org/10.1017/jfm.2026.11138 Published online by Cambridge University Press

Moreover, the Euler equations can be recast as

$$\begin{cases} \nabla\left(\varphi_{1,t}+\dfrac{|\nabla\varphi_1|^2}{2}+\dfrac{P_1}{\rho_1}+gy\right)=0 \quad \text{in} \quad \Omega_1, \\ \nabla\left(\varphi_{2,t}+\dfrac{|\nabla\varphi_2|^2}{2}+\dfrac{P_2}{\rho_2}+gy\right)=0 \quad \text{in} \quad \Omega_2, \\ \nabla\left(\varphi_{3,t}+\dfrac{|\nabla\varphi_3|^2}{2}+\dfrac{P_3}{\rho_3}+gy\right)=0 \quad \text{in} \quad \Omega_3, \end{cases} \tag{2.14}$$

where ∇ denotes the spatial gradient. Thus there are functions $t \mapsto f_i(t),\ i=1,2,3$, such that

$$\begin{cases} \varphi_{1,t}+\dfrac{|\nabla\varphi_1|^2}{2}+\dfrac{P_1}{\rho_1}+gy=f_1(t) \quad \text{in} \quad \Omega_1, \\ \varphi_{2,t}+\dfrac{|\nabla\varphi_2|^2}{2}+\dfrac{P_2}{\rho_2}+gy=f_2(t) \quad \text{in} \quad \Omega_2, \\ \varphi_{3,t}+\dfrac{|\nabla\varphi_3|^2}{2}+\dfrac{P_3}{\rho_3}+gy=f_3(t) \quad \text{in} \quad \Omega_3. \end{cases} \tag{2.15}$$

Utilising the interface conditions (2.5), (2.6) and (2.7), and choosing convenient time-dependent functions $f_1,\ f_2,\ f_3$ in (2.15), we obtain the relations

$$\begin{cases} \rho_1(\varphi_{1,t})_{s_1}+\rho_1\dfrac{|\nabla\varphi_1|^2_{s_1}}{2}+g\rho_1\eta_1=0, \\ \rho_1\left((\varphi_{1,t})_{s_2}+\dfrac{|\nabla\varphi_1|^2_{s_2}}{2}+g\eta_2\right)=\rho_2\left((\varphi_{2,t})_{s_2}+\dfrac{|\nabla\varphi_2|^2_{s_2}}{2}+g\eta_2\right), \\ \rho_2\left((\varphi_{2,t})_{s_3}+\dfrac{|\nabla\varphi_2|^2_{s_3}}{2}+g\eta_3\right)=\rho_3\left((\varphi_{3,t})_{s_3}+\dfrac{|\nabla\varphi_3|^2_{s_3}}{2}+g\eta_3\right). \end{cases} \tag{2.16}$$

One of the main tenets of the Hamiltonian formulation refers to the possibility of reducing the number of the dynamical variables. This feature emerges, using the ansatz by Benjamin & Bridges (1997*a*,*b*) (utilised also by Craig, Guyenne & Sulem 2012). Let us define

$$\begin{aligned} &\Phi^1_1:=\varphi_1(x,h_1+\eta_1(x,t),t)=(\varphi_1)_{s_1}, \quad \Phi^1_2:=\varphi_1(x,\eta_2(x,t),t)=(\varphi_1)_{s_2}, \\ &\Phi^2_2:=\varphi_2(x,\eta_2(x,t),t)=(\varphi_2)_{s_2}, \quad \Phi^2_3:=\varphi_2(x,-h_3+\eta_3(x,t),t)=(\varphi_2)_{s_3}, \\ &\Phi^3:=\varphi_3(x,-h_3+\eta_3(x,t),t)=(\varphi_3)_{s_3}, \\ &\xi_1:=\rho_1\Phi^1_1, \quad \xi_2:=\rho_2\Phi^2_2-\rho_1\Phi^1_2, \quad \xi_3:=\rho_3\Phi^3-\rho_2\Phi^2_3. \end{aligned} \tag{2.17}$$

In what follows, it will be shown that the five traces Φ^i_j can be expressed by the three Hamiltonian 'momenta' ξ_i only. The η_i variables will play the role of Hamiltonian 'coordinates'. This approach reduces not only the number of variables, but also the dimensionality of the problem, because instead of working in the bulk of the fluid (in the two-dimensional spatial domain), one can work only with variables defined on the surfaces and the interfaces, i.e. in one spatial dimension. We note that definition (2.17) arises naturally from the Legendre transform based on the Lagrangian; cf. formula (2.15) in Craig *et al.* (2012).

https://doi.org/10.1017/jfm.2026.11138 Published online by Cambridge University Press

Utilising the notation in (2.17), we obtain from (2.16) that ξ_i satisfy the evolution equations

$$\xi_{1,t} - \rho_1\eta_{1,t}(\varphi_{1,y})_{s_1} + \frac{\rho_1}{2}|\nabla\varphi_1|^2_{s_1} + g\rho_1\eta_1 = 0, \tag{2.18}$$

$$\xi_{2,t} + \eta_{2,t}[\rho_1(\varphi_{1,y})_{s_2} - \rho_2(\varphi_{2,y})_{s_2}] + \rho_2\frac{|\nabla\varphi_2|^2_{s_2}}{2} - \rho_1\frac{|\nabla\varphi_1|^2_{s_2}}{2} + (\rho_2-\rho_1)g\eta_2 = 0, \tag{2.19}$$

$$\xi_{3,t} + \eta_{3,t}[\rho_2(\varphi_{2,y})_{s_3} - \rho_3(\varphi_{3,y})_{s_3}] + \rho_3\frac{|\nabla\varphi_3|^2_{s_3}}{2} - \rho_2\frac{|\nabla\varphi_2|^2_{s_3}}{2} + (\rho_3-\rho_2)g\eta_3 = 0. \tag{2.20}$$

3. The Hamiltonian formulation of the governing equations and the DN operators

In order to alleviate the difficulties brought about by the rich structure of the nonlinear water wave problem, a reformulation of the latter is needed. This is the Hamiltonian formulation that provides a choice of new dependent and independent variables in which the equations take their simplest form.

3.1. *Hamiltonian form of the equations: equations for the moving surfaces*

This subsection is devoted to a reformulation of the governing equations and of the boundary conditions (2.3)–(2.8) by collapsing the dynamical variables into a one-dimensional representation. More precisely, we will rewrite (2.3)–(2.8) as a Hamiltonian system of partial differential equations of the form (cf. Olver 1993)

$$\partial_t\mathfrak{m} = J\frac{\delta H}{\delta\mathfrak{m}}, \tag{3.1}$$

where $t\mapsto\mathfrak{m}(t)$ denotes a path in a Hilbert space $\mathcal{H}$ equipped with an inner product $(\cdot,\cdot)$, and the associated Hamiltonian functional $H:\mathcal{D}\subset\mathcal{H}\to\mathbb{R}$ is defined on a dense subspace $\mathcal{D}$ of $\mathcal{H}$. In our considerations $\mathfrak{m} = (\eta_1,\eta_2,\eta_3,\xi_1,\xi_2,\xi_3)^{\mathrm{T}}$, the Hilbert space is an appropriate Cartesian product of spaces of square-integrable functions and $\mathcal{D} = \mathcal{S}(\mathbb{R})\times\mathcal{S}(\mathbb{R})\times\mathcal{S}(\mathbb{R})\times\mathcal{S}(\mathbb{R})\times\mathcal{S}(\mathbb{R})\times\mathcal{S}(\mathbb{R})$, where $\mathcal{S}(\mathbb{R})$ is the subspace of Schwartz functions in the variable x. Moreover, $J = \begin{pmatrix} 0 & I_3 \\ -I_3 & 0\end{pmatrix}$ (where I_3 is the 3×3 identity matrix) defines a Poisson bracket for functionals by the formula

$$\{F_1, F_2\} = \left(\frac{\delta F_1}{\delta\mathfrak{m}}, J\frac{\delta F_2}{\delta\mathfrak{m}}\right). \tag{3.2}$$

We also denote by $\delta H/\delta\mathfrak{m}$ the variational derivative of H at $\mathfrak{m}\in\mathcal{D}$ through the formula

$$\lim_{\varepsilon\to 0}\frac{H(\mathfrak{m}+\varepsilon\mathfrak{m}_0)-H(\mathfrak{m})}{\varepsilon} = \left(\mathfrak{m}_0, \frac{\delta H}{\delta\mathfrak{m}}\right) \quad \text{for} \quad \mathfrak{m}_0\in\mathcal{D}, \tag{3.3}$$

where $(\cdot,\cdot)$ is the inner product in the Hilbert space $L^2(\mathbb{R})\times L^2(\mathbb{R})\times L^2(\mathbb{R})\times L^2(\mathbb{R})\times L^2(\mathbb{R})\times L^2(\mathbb{R})$.

3.2. *The Hamiltonian functional*

The natural candidate for the Hamiltonian functional is the total energy of the flow given as $E_K + E_P$, where E_K stands for the kinetic energy, and E_P denotes the potential energy.

https://doi.org/10.1017/jfm.2026.11138 Published online by Cambridge University Press

In terms of the quantities of the flow, the kinetic energy is written as

$$E_K = \iint_{\Omega_1\cup\Omega_2\cup\Omega_3} \hat{\rho}\left(\frac{\hat{u}^2+\hat{v}^2}{2}\right) \mathrm{d}y\,\mathrm{d}x, \tag{3.4}$$

which, due to stratification and (2.10), can be detailed as

$$\begin{aligned} E_K &= \int_{\mathbb{R}}\int_{-h}^{-h_3+\eta_3(x,t)} \rho_3\left(\frac{u_3^2+v_3^2}{2}\right)\mathrm{d}y\,\mathrm{d}x + \int_{\mathbb{R}}\int_{-h_3+\eta_3(x,t)}^{\eta_2(x,t)} \rho_2\left(\frac{u_2^2+v_2^2}{2}\right)\mathrm{d}y\,\mathrm{d}x \\ &\quad + \int_{\mathbb{R}}\int_{\eta_2(x,t)}^{h_1+\eta_1(x,t)} \rho_1\left(\frac{u_1^2+v_1^2}{2}\right)\mathrm{d}y\,\mathrm{d}x \\ &= \frac{\rho_3}{2}\int_{\mathbb{R}}\int_{-h}^{-h_3+\eta_3(x,t)} |\nabla\varphi_3|^2\,\mathrm{d}y\,\mathrm{d}x + \frac{\rho_2}{2}\int_{\mathbb{R}}\int_{-h_3+\eta_3(x,t)}^{\eta_2(x,t)} |\nabla\varphi_2|^2\,\mathrm{d}y\,\mathrm{d}x \\ &\quad + \frac{\rho_1}{2}\int_{\mathbb{R}}\int_{\eta_2(x,t)}^{h_1+\eta_1(x,t)} |\nabla\varphi_1|^2\,\mathrm{d}y\,\mathrm{d}x. \end{aligned} \tag{3.5}$$

In defining the potential energy, we act on the realisation that not all the latter energy can be converted into kinetic energy. However, the difference in the potential energy between the perturbed wave state and the pure background state is available for this conversion. Hence we have

$$\begin{aligned} E_P &= g\rho_3\int_{\mathbb{R}}\left(\int_{-h}^{-h_3+\eta_3} y\,\mathrm{d}y - \int_{-h}^{-h_3} y\,\mathrm{d}y\right) + g\rho_2\int_{\mathbb{R}}\left(\int_{-h_3+\eta_3}^{\eta_2} y\,\mathrm{d}y - \int_{-h_3}^{0} y\,\mathrm{d}y\right) \\ &\quad + g\rho_1\int_{\mathbb{R}}\left(\int_{\eta_2}^{h_1+\eta_1} y\,\mathrm{d}y - \int_{0}^{h_1} y\,\mathrm{d}y\right) \\ &= \frac{g\rho_1}{2}\int_{\mathbb{R}}\eta_1^2\,\mathrm{d}x + \frac{g(\rho_2-\rho_1)}{2}\int_{\mathbb{R}}\eta_2^2\,\mathrm{d}x + \frac{g(\rho_3-\rho_2)}{2}\int_{\mathbb{R}}\eta_3^2\,\mathrm{d}x. \end{aligned} \tag{3.6}$$

We note that the above choice for the potential energy allows us to avoid any non-physical constant terms in the energy density and hence infinite energy. More specifically, the potential energy functional (3.6) is not convergent if the potential energy of the pure current background state is not subtracted.

3.3. *Computations of variations of H*

We first list a few useful formulas for computing the variations of H.

REMARK 3.1.

(i) *If* $F(x)=\int_{g_1(x)}^{g_2(x)} f(y)\,\mathrm{d}y$ *for given real functions of one variable* $x\mapsto f(x)$, $x\mapsto g_1(x)$ *and* $x\mapsto g_2(x)$, *then*

$$(\delta F)(x) = \int_{g_1(x)}^{g_2(x)} (\delta f)(y)\,\mathrm{d}y + f(g_2(x))(\delta g_2)(x) - f(g_1(x))(\delta g_1)(x). \tag{3.7}$$

(ii) *For given functions* $(x,\,y)\mapsto F(x,\,y)$, $x\mapsto f_i(x)$ $(i=1,\,2)$, *we have*

$$\begin{aligned} \frac{\partial}{\partial x}\left(\int_{f_1(x)}^{f_2(x)} F(x,\,y)\,\mathrm{d}y\right) &= \int_{f_1(x)}^{f_2(x)} F_x(x,\,y)\,\mathrm{d}y \\ &\quad + F(x,\,f_2(x))\,f_2'(x) - F(x,\,f_1(x))\,f_1'(x). \end{aligned} \tag{3.8}$$

https://doi.org/10.1017/jfm.2026.11138 Published online by Cambridge University Press

(iii) *If θ_1 and θ_2 are harmonic functions satisfying $\nabla\cdot(\theta_1\,\nabla\theta_2)=(\nabla\theta_1)\cdot(\nabla\theta_2)$, then for harmonic variations $\delta\varphi_i$ of φ_i, it holds that*

$$\delta\big((\nabla\varphi_i)\cdot(\nabla\varphi_i)\big)=2\,\nabla\cdot(\delta\varphi_i\,\nabla\varphi_i), \tag{3.9}$$

since $|\nabla\varphi_i|^2=\nabla\cdot(\varphi_i\,\nabla\varphi_i)$ for $i=1,2,3$.

REMARK 3.2. *Regarding variations of the traces on the interfaces of the velocity potentials, the following formulas are true.*

(i) *On the free surface $y=h_1+\eta_1(x,t)$, we have*

$$\begin{aligned}&(\delta\Phi_1^1)(x,t)\\&=\lim_{\varepsilon\to0}\frac{(\varphi_1+\varepsilon\,\delta\varphi_1)\big(x,h_1+\eta_1(x,t)+\varepsilon(\delta\eta_1)(x,t),t\big)-\varphi_1(x,h_1+\eta(x,t),t)}{\varepsilon}\\&=(\varphi_{1,y})_{s_1}\,\delta\eta_1+(\delta\varphi_1)_{s_1}.\end{aligned} \tag{3.10}$$

(ii) *Analogously, on the interface $y=\eta_2(x,t)$, we have*

$$\delta\Phi_2^1=(\varphi_{1,y})_{s_2}\,\delta\eta_2+(\delta\varphi_1)_{s_2}\quad\text{and}\quad\delta\Phi_2^2=(\varphi_{2,y})_{s_2}\,\delta\eta_2+(\delta\varphi_2)_{s_2}. \tag{3.11}$$

(iii) *Finally, on the interface $y=-h_3+\eta_3(x,t)$, we have*

$$\delta\Phi_3^2=(\varphi_{2,y})_{s_3}\,\delta\eta_3+(\delta\varphi_2)_{s_3}\quad\text{and}\quad(\varphi_{3,y})_{s_3}\,\delta\eta_3+(\delta\varphi_3)_{s_3}. \tag{3.12}$$

We proceed now to compute the variations of the terms that make up the kinetic energy E_K from (3.5). Utilising the divergence theorem (Evans 2010), and (3.12) as well as (3.7), (3.8) and (3.9), we obtain

$$\begin{aligned}\delta\left(\int_{\mathbb{R}}\int_{-h}^{-h_3+\eta_3}|\nabla\varphi_3|^2\,\mathrm{d}y\,\mathrm{d}x\right)&=2\int_{\mathbb{R}}(\varphi_{3,y}-\eta_{3,x}\varphi_{3,x})_{s_3}\big(\delta\Phi^3-(\delta\eta_3)(\varphi_{3,y})_{s_3}\big)\mathrm{d}x\\&\quad+\int_{\mathbb{R}}|\nabla\varphi_3|_{s_3}^2\delta\eta_3\,\mathrm{d}x.\end{aligned} \tag{3.13}$$

Analogously, by the same token we have

$$\begin{aligned}\delta\left(\int_{\mathbb{R}}\int_{-h_3+\eta_3}^{\eta_2}|\nabla\varphi_2|^2\,\mathrm{d}y\,\mathrm{d}x\right)&=2\int_{\mathbb{R}}(\varphi_{2,y}-\eta_{2,x}\varphi_{2,x})_{s_2}\big(\delta\Phi_2^2-(\delta\eta_2)(\varphi_{2,y})_{s_2}\big)\mathrm{d}x\\&\quad-2\int_{\mathbb{R}}(\varphi_{2,y}-\eta_{3,x}\varphi_{2,x})_{s_3}\big(\delta\Phi_3^2-(\delta\eta_3)(\varphi_{2,y})_{s_3}\big)\mathrm{d}x\\&\quad+\int_{\mathbb{R}}|\nabla\varphi_2|_{s_2}^2\delta\eta_2\,\mathrm{d}x-\int_{\mathbb{R}}|\nabla\varphi_2|_{s_3}^2\delta\eta_3\,\mathrm{d}x\end{aligned} \tag{3.14}$$

and

$$\begin{aligned}\delta\left(\int_{\mathbb{R}}\int_{\eta_2}^{h_1+\eta_1}|\nabla\varphi_1|^2\,\mathrm{d}y\,\mathrm{d}x\right)&=2\int_{\mathbb{R}}(\varphi_{1,y}-\eta_{1,x}\varphi_{1,x})_{s_1}\big(\delta\Phi_1^1-(\delta\eta_1)(\varphi_{1,y})_{s_1}\big)\mathrm{d}x\\&\quad-2\int_{\mathbb{R}}(\varphi_{1,y}-\eta_{2,x}\varphi_{1,x})_{s_2}\big(\delta\Phi_2^1-(\delta\eta_2)(\varphi_{1,y})_{s_2}\big)\mathrm{d}x\\&\quad+\int_{\mathbb{R}}|\nabla\varphi_1|_{s_1}^2\delta\eta_1\,\mathrm{d}x-\int_{\mathbb{R}}|\nabla\varphi_1|_{s_2}^2\delta\eta_2\,\mathrm{d}x.\end{aligned} \tag{3.15}$$

https://doi.org/10.1017/jfm.2026.11138 Published online by Cambridge University Press

Collecting together the variations of H (from (3.13)–(3.15) and (3.6)) with respect to η_1, η_2 and η_3, respectively, we find that

$$\begin{aligned}\frac{\delta H}{\delta \eta_1} &= -\rho_1\,\eta_{1,t}(\varphi_{1,y})_{s_1} + \frac{\rho_1}{2}|\nabla\varphi_1|^2_{s_1} + g\rho_1\eta_1\\ &= -\rho_1\,\eta_{1,t}(\varphi_{1,y})_{s_1} - \rho_1(\varphi_{1,t})_{s_1}\\ &= -\frac{\mathrm{d}}{\mathrm{d}t}\left(\rho_1\,\varphi_1(x, h_1+\eta_1(x,t),t)\right)\\ &= -\xi_{1,t},\end{aligned} \tag{3.16}$$

$$\begin{aligned}\frac{\delta H}{\delta \eta_2} &= \rho_1\,\eta_{2,t}(\varphi_{1,y})_{s_2} - \frac{\rho_1}{2}|\nabla\varphi_1|^2_{s_2} - \rho_2\,\eta_{2,t}(\varphi_{2,y})_{s_2} + \frac{\rho_2}{2}|\nabla\varphi_2|^2_{s_2} + (\rho_2-\rho_1)g\eta_2\\ &= -\rho_2\left((\varphi_{2,t})_{s_2} + \eta_{2,t}(\varphi_{2,y})_{s_2}\right) + \rho_1\left((\varphi_{1,t})_{s_2} + \eta_{2,t}(\varphi_{1,y})_{s_2}\right)\\ &= -\frac{\mathrm{d}}{\mathrm{d}t}\left(\rho_2\,\varphi_2(x,\eta_2(x,t),t)\right) + \frac{\mathrm{d}}{\mathrm{d}t}\left(\rho_1\,\varphi_1(x,\eta_2(x,t),t)\right)\\ &= -\xi_{2,t}\end{aligned} \tag{3.17}$$

and

$$\begin{aligned}\frac{\delta H}{\delta \eta_3} &= \rho_2\,\eta_{3,t}(\varphi_{2,y})_{s_3} - \frac{\rho_2}{2}|\nabla\varphi_2|^2_{s_3} - \rho_3\,\eta_{3,t}(\varphi_{3,y})_{s_3} + \frac{\rho_3}{2}|\nabla\varphi_3|^2_{s_3} + (\rho_3-\rho_2)g\eta_3\\ &= -\rho_3\left((\varphi_{3,t})_{s_3} + \eta_{3,t}(\varphi_{3,y})_{s_3}\right) + \rho_2\left((\varphi_{2,t})_{s_3} + \eta_{3,t}(\varphi_{2,y})_{s_3}\right)\\ &= -\frac{\mathrm{d}}{\mathrm{d}t}\left(\rho_3\,\varphi_3(x,-h_3+\eta_3(x,t),t)\right) + \frac{\mathrm{d}}{\mathrm{d}t}\left(\rho_2\,\varphi_2(x,-h_3+\eta_3(x,t),t)\right)\\ &= -\xi_{3,t}.\end{aligned} \tag{3.18}$$

Moreover, glancing at (2.17) and utilising (3.13)–(3.15), we infer that

$$\frac{\delta H}{\delta \xi_1} = \eta_{1,t}, \quad \frac{\delta H}{\delta \xi_2} = \eta_{2,t}, \quad \frac{\delta H}{\delta \xi_3} = \eta_{3,t}. \tag{3.19}$$

We summarise the conclusions regarding the variations of H computed in (3.16), (3.17), (3.18) and (3.19) in the following theorem.

THEOREM 3.3. *The governing equations and boundary conditions (2.3)–(2.8) possess the Hamiltonian formulation*

$$\begin{cases}\dfrac{\delta H}{\delta \eta_1} = -\xi_{1,t}, & \dfrac{\delta H}{\delta \xi_1} = \eta_{1,t},\\[2mm] \dfrac{\delta H}{\delta \eta_2} = -\xi_{2,t}, & \dfrac{\delta H}{\delta \xi_2} = \eta_{2,t},\\[2mm] \dfrac{\delta H}{\delta \eta_3} = -\xi_{3,t}, & \dfrac{\delta H}{\delta \xi_3} = \eta_{3,t}.\end{cases} \tag{3.20}$$

REMARK 3.4. *The (equivalent) Hamiltonian (re)formulation of the water wave problem not only reduces the number of the dynamical variables, but (together with the DN machinery) also offers the possibility to derive (simpler) nonlinear model equations directly from the full nonlinear water waves equations in multi-layer flows with a free surface. As a result, the coefficients in these equations (and also their solutions) depend explicitly on physical parameters on the multi-layer system; cf. Craig et al. (2005, 2012) and Constantin & Ivanov (2019). More precisely, from a single overarching principle – the Hamiltonian formulation – one can derive model equations pertaining to various*

https://doi.org/10.1017/jfm.2026.11138 Published online by Cambridge University Press

physical regimes by simply defining suitable scaling regimes in terms of certain ratios such as amplitude/layer depth and/or amplitude/wavelength; cf. e.g. Craig et al. (2005, 2012) and Constantin & Ivanov (2019). This is in stark contrast to the usual case-by-case analysis (Whitham 1999). Furthermore, the Hamiltonian perspective is very suited to perturbation analysis since it guarantees that if appropriate symmetries are preserved in the approximation process, then conservation properties of the exact system are retained in its approximations.

3.4. *The DN operators*

The DN operator corresponding to the uppermost layer is defined as

$$\begin{pmatrix} G_{11} & G_{12} \\ G_{21} & G_{22} \end{pmatrix} \begin{pmatrix} (\varphi_1)_{s_2} \\ (\varphi_1)_{s_1} \end{pmatrix} = \begin{pmatrix} -\sqrt{1+\eta_{2,x}^2}\left(\dfrac{\partial \varphi_1}{\partial \boldsymbol{n}_2}\right)_{s_2} \\ \sqrt{1+\eta_{1,x}^2}\left(\dfrac{\partial \varphi_1}{\partial \boldsymbol{n}_1}\right)_{s_1} \end{pmatrix}, \tag{3.21}$$

where $\boldsymbol{n}_2 = (-\eta_{2,x}, 1)/\sqrt{1+\eta_{2,x}^2}$ and $\boldsymbol{n}_1 = (-\eta_{1,x}, 1)/\sqrt{1+\eta_{1,x}^2}$ are the unit normal vectors to the upper interface $y = \eta_2(x,t)$ and to the top surface $y = -h_1 + \eta_1(x,t)$, respectively. The DN operator corresponding to the middle layer is

$$\begin{pmatrix} \Gamma_{11} & \Gamma_{12} \\ \Gamma_{21} & \Gamma_{22} \end{pmatrix} \begin{pmatrix} (\varphi_2)_{s_2} \\ (\varphi_2)_{s_3} \end{pmatrix} = \begin{pmatrix} \sqrt{1+\eta_{2,x}^2}\left(\dfrac{\partial \varphi_2}{\partial \boldsymbol{n}_2}\right)_{s_2} \\ -\sqrt{1+\eta_{3,x}^2}\left(\dfrac{\partial \varphi_2}{\partial \boldsymbol{n}_3}\right)_{s_3} \end{pmatrix}, \tag{3.22}$$

where $\boldsymbol{n}_3 = (-\eta_{3,x}, 1)/\sqrt{1+\eta_{3,x}^2}$ denotes the outward pointing unit normal vector corresponding to the lower interface $y = -h_3 + \eta_3(x,t)$. Moreover, the DN operator corresponding to the bottom layer is

$$G(\eta_3)(\varphi_3)_{s_3} = \sqrt{1+\eta_{3,x}^2}\,(\partial\varphi_3/\partial \boldsymbol{n}_3)_{s_3} = (\nabla\varphi_3)_{s_3} \cdot (-\eta_{3,x}, 1). \tag{3.23}$$

These DN operators for each domain $\Omega_1, \Omega_2, \Omega_3$ could be obtained recursively in the form of asymptotic series in η_1, η_2, η_3 following the technique described in the Appendix of Craig *et al.* (2005); see also Appendix A of Ivanov, Martin & Todorov (2022).

Appealing to the divergence theorem (Evans 2010), the kinetic energy of the system (3.5) can be rewritten as

$$\begin{aligned} \mathrm{E}_K = {} & \frac{\rho_1}{2}\int (\varphi_1)_{s_1}\,(\nabla\varphi_1)_{s_1} \cdot (-\eta_{1,x}, 1)\,\mathrm{d}x - \frac{\rho_1}{2}\int (\varphi_1)_{s_2}\,(\nabla\varphi_1)_{s_2} \cdot (-\eta_{2,x}, 1)\,\mathrm{d}x \\ & + \frac{\rho_2}{2}\int (\varphi_2)_{s_2}\,(\nabla\varphi_2)_{s_2} \cdot (-\eta_{2,x}, 1)\,\mathrm{d}x - \frac{\rho_2}{2}\int (\varphi_2)_{s_3}\,(\nabla\varphi_2)_{s_3} \cdot (-\eta_{3,x}, 1)\,\mathrm{d}x \\ & + \frac{\rho_3}{2}\int (\varphi_3)_{s_3}\,(\nabla\varphi_3)_{s_3} \cdot (-\eta_{3,x}, 1)\,\mathrm{d}x. \end{aligned} \tag{3.24}$$

With the help of the DN operators, the kinetic energy can be written as

$$\begin{aligned} \mathrm{E}_K = {} & \frac{\rho_1}{2}\int (\varphi_1)_{s_1}\left[G_{21}(\varphi_1)_{s_2} + G_{22}(\varphi_1)_{s_1}\right]\mathrm{d}x \\ & + \frac{\rho_1}{2}\int (\varphi_1)_{s_2}\left[G_{11}(\varphi_1)_{s_2} + G_{12}(\varphi_1)_{s_1}\right]\mathrm{d}x \end{aligned}$$

https://doi.org/10.1017/jfm.2026.11138 Published online by Cambridge University Press

$$+\frac{\rho_2}{2}\int (\varphi_2)_{s_2}\left[\Gamma_{11}(\varphi_2)_{s_2}+\Gamma_{12}(\varphi_2)_{s_3}\right]\,\mathrm{d}x$$
$$+\frac{\rho_2}{2}\int (\varphi_2)_{s_3}\left[\Gamma_{21}(\varphi_2)_{s_2}+\Gamma_{22}(\varphi_2)_{s_3}\right]\,\mathrm{d}x$$
$$+\frac{\rho_3}{2}\int (\varphi_3)_{s_3}G(\eta_3)(\varphi_3)_{s_3}\,\mathrm{d}x. \tag{3.25}$$

Attempting to simplify (3.25) we note first that from the kinematic condition at the upper interface $y=\eta_2(x,t)$, we have

$$\eta_{2,t}=(\nabla\varphi_2)_{s_2}\cdot(\eta_{2,x},-1)=(\nabla\varphi_1)_{s_2}\cdot(\eta_{2,x},-1), \tag{3.26}$$

which, in terms of the DN operators, becomes

$$\eta_{2,t}=-(\Gamma_{11}(\varphi_2)_{s_2}+\Gamma_{12}(\varphi_2)_{s_3})=G_{11}(\varphi_1)_{s_2}+G_{12}(\varphi_1)_{s_1}. \tag{3.27}$$

Moreover,

$$\eta_{3,t}=(\varphi_{2,y}-\varphi_{2,x}\eta_{3,x})_{s_3}=(\varphi_{3,y}-\varphi_{3,x}\eta_{3,x})_{s_3}, \tag{3.28}$$

which implies

$$\eta_{3,t}=G(\eta_3)(\varphi_3)_{s_3}=-\left[\Gamma_{21}(\varphi_2)_{s_2}+\Gamma_{22}(\varphi_2)_{s_3}\right]. \tag{3.29}$$

Recalling that

$$\xi_1=\rho_1(\varphi_1)_{s_1},\quad \xi_2=\rho_2(\varphi_2)_{s_2}-\rho_1(\varphi_1)_{s_2},\quad \xi_3=\rho_3(\varphi_3)_{s_3}-\rho_2(\varphi_2)_{s_3}, \tag{3.30}$$

and employing (3.27) and (3.29), we see that the kinetic energy can be simplified as

$$E_K=\frac{1}{2}\int \xi_1\left[G_{21}(\varphi_1)_{s_2}+G_{22}(\varphi_1)_{s_1}\right]\,\mathrm{d}x$$
$$+\frac{1}{2}\int \xi_2\left[\Gamma_{11}(\varphi_2)_{s_2}+\Gamma_{12}(\varphi_2)_{s_3}\right]\,\mathrm{d}x \tag{3.31}$$
$$+\frac{1}{2}\int \xi_3\,G(\eta_3)(\varphi_3)_{s_3}\,\mathrm{d}x.$$

Moreover, from (3.27) and (3.29), we also obtain the system

$$\xi_2=\rho_2(\varphi_2)_{s_2}+\rho_1G_{11}^{-1}[\Gamma_{11}(\varphi_2)_{s_2}+\Gamma_{12}(\varphi_2)_{s_3}+\rho_1^{-1}G_{12}\xi_1], \tag{3.32}$$

$$\xi_3=-\rho_2(\varphi_2)_{s_3}-\rho_3\,G^{-1}(\eta_3)\,[\Gamma_{21}(\varphi_2)_{s_2}+\Gamma_{22}(\varphi_2)_{s_3}], \tag{3.33}$$

which can be rearranged as

$$\begin{aligned}(\rho_2+\rho_1G_{11}^{-1}\Gamma_{11})(\varphi_2)_{s_2}+(\rho_1G_{11}^{-1}\Gamma_{12})(\varphi_2)_{s_3}&=\xi_2-G_{11}^{-1}G_{12}\xi_1,\\ (-\rho_3\,G^{-1}(\eta_3)\,\Gamma_{21})(\varphi_2)_{s_2}-(\rho_2+\rho_3\,G^{-1}(\eta_3)\,\Gamma_{22})(\varphi_2)_{s_3}&=\xi_3,\end{aligned} \tag{3.34}$$

where the superscript -1 in the previous system (and in the subsequent equations) is used to refer to the inverse of the operator in question.

Taking into account the fact that (3.34) is a linear system of equations with operator-valued coefficients, we obtain

$$\begin{aligned}(\varphi_2)_{s_2}&=\mathcal{D}^{-1}\big(\rho_1G\xi_3+(\rho_2G+\rho_3\Gamma_{22})\Gamma_{12}^{-1}(G_{11}\xi_2-G_{12}\xi_1)\big)\equiv\Phi_2^2(\eta_i,\xi_i),\\ (\varphi_2)_{s_3}&=-(\mathcal{D}^*)^{-1}\big(\rho_3(G_{11}\xi_2-G_{12}\xi_1)+(\rho_2G_{11}+\rho_1\Gamma_{11})\Gamma_{21}^{-1}G\xi_3\big),\end{aligned} \tag{3.35}$$

where $\mathcal{D}:=((\rho_2G+\rho_3\Gamma_{22})\Gamma_{12}^{-1}(\rho_2G_{11}+\rho_1\Gamma_{11})-\rho_1\rho_3\Gamma_{21})$, and the star $(*)$ notation denotes the operation of conjugation. (The conjugation is with respect to the standard real

https://doi.org/10.1017/jfm.2026.11138 Published online by Cambridge University Press

bilinear form $(f,\,g)=\int_{\mathbb{R}} f(x)\,g(x)\,\mathrm{d}x$.) We used also the fact that $G_{ij}=G_{ji}^{*}$ and $\Gamma_{ij}=\Gamma_{ji}^{*}$; see e.g. Craig *et al.* (2005). Moreover, from (3.30), we also have

$$\begin{aligned}(\varphi_1)_{s_2}&=\frac{1}{\rho_1}\mathcal{D}^{-1}\big(\rho_1(\rho_2 G\xi_3+\rho_3\Gamma_{21}\xi_2)-(\rho_2 G+\rho_3\Gamma_{22})\Gamma_{12}^{-1}(\rho_2 G_{12}\xi_1+\rho_1\Gamma_{11}\xi_2)\big)\\&\equiv\Phi_2^1(\eta_i,\xi_i),\\(\varphi_3)_{s_3}&=-(\mathcal{D}^{*})^{-1}\big(\rho_2 G_{11}\xi_2-\rho_2 G_{12}\xi_1+\rho_1\Gamma_{12}\xi_3-(\rho_2 G_{11}+\rho_1\Gamma_{11})\Gamma_{21}^{-1}\Gamma_{22}\xi_3\big).\end{aligned}\tag{3.36}$$

The previous expressions of the surface values of the potentials together with (3.6) allow us to express the Hamiltonian as a functional of the quantities η_i, ξ_i $(i=1,\,2,\,3)$, i.e. we have

$$\begin{aligned}H&=E_K(\xi_i)+V(\eta_i)\\&=\frac{1}{2}\int\xi_1 A_{11}\xi_1\,\mathrm{d}x+\frac{1}{2}\int\xi_2 A_{22}\xi_2\,\mathrm{d}x+\frac{1}{2}\int\xi_3 A_{33}\xi_3\,\mathrm{d}x\\&\quad+\int\xi_1 A_{12}\xi_2\,\mathrm{d}x+\int\xi_1 A_{13}\xi_3\,\mathrm{d}x+\int\xi_2 A_{23}\xi_3\,\mathrm{d}x\\&\quad+\frac{1}{2}\int\big(g\rho_1\eta_1^2+g(\rho_2-\rho_1)\eta_2^2+g(\rho_3-\rho_2)\eta_3^2\big)\,\mathrm{d}x,\end{aligned}\tag{3.37}$$

where the last integral is the potential energy V, and the operators A_{ij} $(i,\,j=1,\,2,\,3)$, written in terms of the DN operators, are

$$\begin{aligned}A_{11}&=\frac{1}{\rho_1}G_{22}-\frac{\rho_2}{\rho_1}G_{21}\mathcal{D}^{-1}(\rho_2 G+\rho_3\Gamma_{22})\Gamma_{12}^{-1}G_{12},\\A_{22}&=\Gamma_{11}\mathcal{D}^{-1}(\rho_2 G+\rho_3\Gamma_{22})\Gamma_{12}^{-1}G_{11}-\rho_3 G_{11}\mathcal{D}^{-1}\Gamma_{21},\\A_{33}&=\big(\Gamma_{22}\Gamma_{12}^{-1}(\rho_2 G_{11}+\rho_1\Gamma_{11})-\rho_1\Gamma_{21}\big)\mathcal{D}^{-1}G,\\A_{12}&=\rho_3 G_{21}\mathcal{D}^{-1}\Gamma_{21}-\frac{1}{2}G_{21}\big(\mathcal{D}^{-1}(\rho_2 G+\rho_3\Gamma_{22})\Gamma_{12}^{-1}+\Gamma_{21}^{-1}(\rho_2 G+\rho_3\Gamma_{22})(\mathcal{D}^{*})^{-1}\big)\Gamma_{11},\\A_{13}&=\frac{1}{2}\rho_2 G_{21}\big(\mathcal{D}^{-1}+(\mathcal{D}^{*})^{-1}\big)G,\\A_{23}&=\frac{1}{2}\big((\rho_1\Gamma_{11}-\rho_2 G_{11})\mathcal{D}^{-1}-\Gamma_{12}(\mathcal{D}^{*})^{-1}(\rho_2 G_{11}+\rho_1\Gamma_{11})\Gamma_{21}^{-1}\big)G.\end{aligned}\tag{3.38}$$

The Hamiltonian equations can be represented, via the DN operators, with the help of the quantities $(\varphi_{1,x}(x,\,y,\,t))_{s_1}$ and $(\varphi_{1,y}(x,\,y,\,t))_{s_1}$. From (3.37) and because the operators A_{ij} do not depend on ξ_i, we obtain (in terms of the Hamiltonian variables) the evolution equation

$$\eta_{1,t}=\frac{\delta H}{\delta\xi_1}=A_{11}\xi_1+A_{12}\xi_2+A_{13}\xi_3:=F_1(\eta_i,\xi_i).\tag{3.39}$$

In addition, by (3.37) and (3.20), $(\varphi_{1,x}(x,\,y,\,t))_{s_1}$ and $(\varphi_{1,y}(x,\,y,\,t))_{s_1}$ satisfy the system

$$\begin{aligned}&(\varphi_{1,x})_{s_1}+(\varphi_{1,y})_{s_1}\eta_{1,x}=\frac{1}{\rho_1}\xi_{1,x},\\&(\varphi_{1,y})_{s_1}-(\varphi_{1,x})_{s_1}\eta_{1,x}=\eta_{1,t}=F_1(\eta_i,\xi_i).\end{aligned}\tag{3.40}$$

https://doi.org/10.1017/jfm.2026.11138 Published online by Cambridge University Press

Solving the system, we find

$$(\varphi_{1,x})_{s_1} = \frac{\xi_{1,x} - \rho_1 \eta_{1,x} F_1}{\rho_1 \left(1 + \eta_{1,x}^2\right)},$$
$$(\varphi_{1,y})_{s_1} = \frac{\eta_{1,x} \xi_{1,x} + \rho_1 F_1}{\rho_1 \left(1 + \eta_{1,x}^2\right)}, \tag{3.41}$$

which allow us to write (2.18) through the Hamiltonian variables. More precisely, we have

$$\xi_{1,t} + \frac{\xi_{1,x}^2 - 2\rho_1 \eta_{1,x} \xi_{1,x} F_1 - \rho_1^2 F_1^2}{2\rho_1 \left(1 + \eta_{1,x}^2\right)} + g\rho_1 \eta_1 = 0. \tag{3.42}$$

The counterpart equation for η_1 is of course (3.39),

$$\eta_{1,t} = F_1(\xi_i, \eta_i). \tag{3.43}$$

From (3.37), where the operators A_{ij} do not depend on ξ_i, we have

$$\eta_{2,t} = \frac{\delta H}{\delta \xi_2} = A_{12}^* \xi_1 + A_{22} \xi_2 + A_{23} \xi_3 =: F_2(\eta_i, \xi_i). \tag{3.44}$$

Thus $F_2(\eta_i, \xi_i)$ is defined through the canonical variables. Next, from (3.35) we have $(\varphi_2)_{s_2} \equiv \Phi_2^2(\eta_i, \xi_i)$ as a known quantity, defined through the canonical variables. Since

$$\frac{\mathrm{d}}{\mathrm{d}x} \Phi_2^2 = (\varphi_{2,x})_{s_2} + (\varphi_{2,y})_{s_2} \eta_{2,x}, \tag{3.45}$$

and from (2.12)

$$F_2 = \eta_{2,t} = (\varphi_{2,y})_{s_2} - (\varphi_{2,x})_{s_2} \eta_{2,x}, \tag{3.46}$$

we have a system

$$(\varphi_{2,x})_{s_2} + \eta_{2,x} (\varphi_{2,y})_{s_2} = (\Phi_2^2)_x, \tag{3.47}$$
$$-\eta_{2,x} (\varphi_{2,x})_{s_2} + (\varphi_{2,y})_{s_2} = F_2, \tag{3.48}$$

which gives

$$(\varphi_{2,x})_{s_2} = \frac{(\Phi_2^2)_x - \eta_{2,x} F_2}{1 + \eta_{2,x}^2}, \tag{3.49}$$

$$(\varphi_{2,y})_{s_2} = \frac{\eta_{2,x} (\Phi_2^2)_x + F_2}{1 + \eta_{2,x}^2}, \tag{3.50}$$

and similarly,

$$(\varphi_{1,x})_{s_2} = \frac{(\Phi_2^1)_x - \eta_{2,x} F_2}{1 + \eta_{2,x}^2}, \tag{3.51}$$

$$(\varphi_{1,y})_{s_2} = \frac{\eta_{2,x} (\Phi_2^1)_x + F_2}{1 + \eta_{2,x}^2}, \tag{3.52}$$

https://doi.org/10.1017/jfm.2026.11138 Published online by Cambridge University Press

where Φ_2^1 is defined in (3.36). Therefore, ξ_2 satisfies the equation

$$\xi_{2,t} + \frac{\rho_2(\Phi^2_{2,x})^2 - \rho_1(\Phi^1_{2,x})^2 - 2F_2\xi_{2,x}\eta_{2,x} + (\rho_1 - \rho_2)F_2^2}{2\big(1+\eta^2_{2,x}\big)} + (\rho_2 - \rho_1)g\eta_2 = 0. \tag{3.53}$$

Similarly, for the last pair of equations, we obtain

$$\eta_{3,t} = \frac{\delta H}{\delta \xi_3} = A^*_{13}\xi_1 + A^*_{23}\xi_2 + A_{33}\xi_3 := F_3(\eta_i, \xi_i) \tag{3.54}$$

and

$$\xi_{3,t} + \frac{\rho_3(\Phi^3_x)^2 - \rho_2(\Phi^2_{3,x})^2 - 2F_3\xi_{3,x}\eta_{3,x} + (\rho_2 - \rho_3)F_3^2}{2\big(1+\eta^2_{3,x}\big)} + (\rho_3 - \rho_2)g\eta_3 = 0. \tag{3.55}$$

We note that (3.42), (3.53), (3.55), (3.43), (3.44), (3.54) render a closed system of six equations for the six variables (η_i, ξ_i), $i = 1, 2, 3$. All quantities in these equations are given in terms of the DN operators. Most importantly, (3.42), (3.53), (3.55), (3.43), (3.44), (3.54) also suggest the pattern for more superimposed layers.

4. The DN operators and the dispersion relation

4.1. *The derivation of the dispersion relation*

A significant role in the derivation of the dispersion relation will be played by the DN operators introduced in (3.21), (3.22) and (3.23). The DN operators are analytic in their dependence on (η_1, η_2), (η_2, η_3) and η_3, respectively, and have convergent Taylor series expansions

$$\begin{pmatrix} G_{11}(\eta_1,\eta_2) & G_{12}(\eta_1,\eta_2) \\ G_{21}(\eta_1,\eta_2) & G_{22}(\eta_1,\eta_2) \end{pmatrix} = \sum_{k_1,k_2=0}^{\infty} \begin{pmatrix} G_{11}^{(k_1k_2)}(\eta_1,\eta_2) & G_{12}^{(k_1k_2)}(\eta_1,\eta_2) \\ G_{21}^{(k_1k_2)}(\eta_1,\eta_2) & G_{22}^{(k_1k_2)}(\eta_1,\eta_2) \end{pmatrix}, \tag{4.1}$$

$$\begin{pmatrix} \Gamma_{11}(\eta_2,\eta_3) & \Gamma_{12}(\eta_2,\eta_3) \\ \Gamma_{21}(\eta_2,\eta_3) & \Gamma_{22}(\eta_2,\eta_3) \end{pmatrix} = \sum_{p_1,p_2=0}^{\infty} \begin{pmatrix} \Gamma_{11}^{(p_2p_3)}(\eta_2,\eta_3) & \Gamma_{12}^{(p_2p_3)}(\eta_2,\eta_3) \\ \Gamma_{21}^{(p_2p_3)}(\eta_2,\eta_3) & \Gamma_{22}^{(p_2p_3)}(\eta_2,\eta_3) \end{pmatrix}, \tag{4.2}$$

$$G(\eta_3) = \sum_{l=0}^{\infty} G^{(l)}(\eta_3), \tag{4.3}$$

with each linear operator $G_{ij}^{(k_1k_2)}(\eta_1, \eta_2)$ homogeneous of degree k_1 in η_1, and of degree k_2 in η_2, for $i, j = 1, 2$, each linear operator $\Gamma_{ij}^{(p_2p_3)}(\eta_2, \eta_3)$ homogeneous of degree p_2 in η_2, and of degree p_3 in η_3, for $i, j = 1, 2$, and each linear operator $G^{(l)}(\eta_3)$ homogeneous of degree l in η_3; cf. Craig *et al.* (2005, 2012). Each of the operators $G_{ii}^{(k_1k_2)}(\eta_1, \eta_2)$ with $i = 1, 2$ and $k_1, k_2 \geq 0$, $\Gamma_{ii}^{(p_2p_3)}(\eta_2, \eta_3)$ with $i = 1, 2$ and $p_1, p_2 \geq 0$, and $G^{(l)}(\eta_3)$ with $l \geq 0$, is self-adjoint.

REMARK 4.1. *The DN operators can be understood as certain pseudo-differential operators. More precisely, letting m be a complex-valued function of a real variable whose*

https://doi.org/10.1017/jfm.2026.11138 Published online by Cambridge University Press

derivatives of any order have polynomial growth, and setting

$$D := -i\,\partial_x, \tag{4.4}$$

we define

$$(m(D)f)(x) := \frac{1}{2\pi}\iint \mathrm{e}^{\mathrm{i}k(x-y)}\, m(k)\, f(y)\,\mathrm{d}y\,\mathrm{d}k. \tag{4.5}$$

The operator $m(D)$ is called a Fourier multiplier operator and maps $\mathcal{S}(\mathbb{R})$ into $\mathcal{S}(\mathbb{R})$. Furthermore,

(i) *$m(D)$ extends to a self-adjoint operator in $L^2(\mathbb{R})$ if and only if m is real valued (cf. Reed & Simon 1975)*
(ii) *$m(D)$ is bounded if and only if $m \in L^\infty(\mathbb{R})$.*

Then the leading-order terms of the DN operators are given (cf. Craig *et al.* 2005) by means of Fourier multipliers as

$$\begin{pmatrix} G^0_{11} & G^0_{12} \\ G^0_{21} & G^0_{22} \end{pmatrix} = \begin{pmatrix} D\coth(h_1 D) & -D\,\mathrm{csch}(h_1 D) \\ -D\,\mathrm{csch}(h_1 D) & D\coth(h_1 D) \end{pmatrix}, \tag{4.6}$$

$$\begin{pmatrix} \Gamma^0_{11} & \Gamma^0_{12} \\ \Gamma^0_{21} & \Gamma^0_{22} \end{pmatrix} = \begin{pmatrix} D\coth(h_3 D) & -D\,\mathrm{csch}(h_3 D) \\ -D\,\mathrm{csch}(h_3 D) & D\coth(h_3 D) \end{pmatrix} \tag{4.7}$$

and

$$G^0 = D\tanh(h_b D), \tag{4.8}$$

where $h_b := h - h_3$ is the mean depth of the bottom layer, for h_3 the mean depth of the middle layer.

Under consideration will be monochromatic solutions of the leading-order linear equations, meaning that all components of these solutions are proportional to $\exp(ikx)$, where $k := 2\pi/L$ represents the wavenumber, L being the corresponding wavelength. The latter means that each component is an eigenfunction of the operator D with eigenvalue k. These facts allow us to replace the operator D by its eigenvalue k when acting on the previously mentioned monochromatic solutions. Consequently, leading-order approximations of the operators $A_{ij}(k)$ $(i,\, j = 1,\, 2,\, 3)$, which are denoted by $A^0_{ij}(k)$ $(i,\, j = 1,\, 2,\, 3)$, acquire the form

$$\begin{aligned}
A^0_{11}(k) &= \frac{k}{\rho_1}\coth(kh_1) - \frac{k\rho_2\big(\rho_3\cosh(kh_3)\cosh(kh_b) + \rho_2\sinh(kh_3)\sinh(kh_b)\big)}{\rho_1\sinh(kh_1)\,\Delta(k)}, \\
A^0_{22}(k) &= \frac{k}{\Delta(k)}\cosh(kh_1)\big(\rho_2\cosh(kh_3)\sinh(kh_b) + \rho_3\sinh(kh_3)\cosh(kh_b)\big), \\
A^0_{33}(k) &= \frac{k}{\Delta(k)}\sinh(kh_b)\big(\rho_1\sinh(kh_1)\sinh(kh_3) + \rho_2\cosh(kh_3)\cosh(kh_1)\big), \\
A^0_{12}(k) &= \frac{k}{\Delta(k)}\big(\rho_2\cosh(kh_3)\sinh(kh_b) + \rho_3\sinh(kh_3)\cosh(kh_b)\big), \\
A^0_{13}(k) &= \frac{k\rho_2}{\Delta(k)}\sinh(kh_b), \\
A^0_{23}(k) &= \frac{k\rho_2}{\Delta(k)}\sinh(kh_b)\cosh(kh_1),
\end{aligned} \tag{4.9}$$

https://doi.org/10.1017/jfm.2026.11138 Published online by Cambridge University Press

where

$$\begin{aligned}\Delta(k) = {}& \rho_2\big(\rho_3\cosh(kh_3)\cosh(kh_b) + \rho_2\sinh(kh_3)\sinh(kh_b)\big)\cosh(kh_1)\\ &+ \rho_1\big(\rho_2\cosh(kh_3)\sinh(kh_b) + \rho_3\sinh(kh_3)\cosh(kh_b)\big)\sinh(kh_1).\end{aligned} \tag{4.10}$$

Note that

$$\begin{aligned}\Delta(k) &> \rho_1^2\big(\cosh(kh_3)\cosh(kh_b) + \sinh(kh_3)\sinh(kh_b)\big)\cosh(kh_1)\\ &\quad + \rho_1^2\big(\cosh(kh_3)\sinh(kh_b) + \sinh(kh_3)\cosh(kh_b)\big)\sinh(kh_1)\\ &= \rho_1^2\big(\cosh(kh_3 + kh_b)\cosh(kh_1) + \sinh(kh_3 + kh_b)\sinh(kh_1)\big)\\ &= \rho_1^2\cosh(k(h_3 + h_b + h_1)) = \rho_1^2\cosh(k(h + h_1)) > 0.\end{aligned} \tag{4.11}$$

We observe that in the leading order, all $A^0_{ij}(k)$ are even functions of k, therefore the operators $A^0_{ij}(D)$ are self-conjugate operators. Thus from (3.39), (3.44) and (3.54), we have

$$\begin{aligned}\eta_{1,t} &= A^0_{11}(D)\,\xi_1 + A^0_{12}(D)\,\xi_2 + A^0_{13}(D)\,\xi_3,\\ \eta_{2,t} &= A^0_{12}(D)\,\xi_1 + A^0_{22}(D)\,\xi_2 + A^0_{23}(D)\,\xi_3,\\ \eta_{3,t} &= A^0_{13}(D)\,\xi_1 + A^0_{23}(D)\,\xi_2 + A^0_{33}(D)\,\xi_3.\end{aligned} \tag{4.12}$$

On the other hand, retaining only the linear terms in (3.42), (3.53) and (3.55), we obtain the equations

$$\begin{aligned}\xi_{1,t} &= -g\rho_1\eta_1,\\ \xi_{2,t} &= -g(\rho_2 - \rho_1)\eta_2,\\ \xi_{3,t} &= -g(\rho_3 - \rho_2)\eta_3.\end{aligned} \tag{4.13}$$

Denoting now $\mathfrak{m} = (\eta_1, \eta_2, \eta_3, \xi_1, \xi_2, \xi_3)^{\mathrm{T}}$, we will solve the linear system (4.12)–(4.13) by utilising the Fourier transform: setting $\hat{f}(k) = (1/\sqrt{2\pi})\int_{\mathbb{R}} \mathrm{e}^{-\mathrm{i}kx} f(x)\,\mathrm{d}x$ for $f \in \mathcal{S}(\mathbb{R})$, in each component of $\mathfrak{m}$, we see (after taking into account (3.20), (3.37) and (4.13)) that the system (3.20) is transformed for any fixed $k \in \mathbb{R}$ into the linear autonomous system of ordinary differential equations

$$\partial_t\hat{\mathfrak{m}}(k, t) = \mathcal{M}(k)\,\hat{\mathfrak{m}}(k, t), \tag{4.14}$$

where

$$\mathcal{M}(k) = \begin{pmatrix} 0 & 0 & 0 & A^0_{11}(k) & A^0_{12}(k) & A^0_{13}(k)\\ 0 & 0 & 0 & A^0_{12}(k) & A^0_{22}(k) & A^0_{23}(k)\\ 0 & 0 & 0 & A^0_{13}(k) & A^0_{23}(k) & A^0_{33}(k)\\ -g\rho_1 & 0 & 0 & 0 & 0 & 0\\ 0 & g(\rho_1 - \rho_2) & 0 & 0 & 0 & 0\\ 0 & 0 & g(\rho_2 - \rho_3) & 0 & 0 & 0 \end{pmatrix}. \tag{4.15}$$

REMARK 4.2. *According to Constantin & Ivanov (2019), the unique solution to (4.14) is given by* $\hat{\mathfrak{m}}(k, t) = e^{\mathcal{M}(k)\,t}\,\hat{\mathfrak{m}}_0(k)$ *(where* $\mathfrak{m}_0(k) = (1/\sqrt{2\pi})\int_{\mathbb{R}} \mathfrak{m}_0(x)\,\mathrm{e}^{\mathrm{i}kx}\,\mathrm{d}x$ *are the initial data) and corresponds (via the inverse Fourier transform) to the solution*

$$\mathfrak{m}(x, t) = \frac{1}{2\pi}\int_{\mathbb{R}} e^{\mathcal{M}(k)\,t}\,\hat{\mathfrak{m}}_0(k)\,\mathrm{e}^{\mathrm{i}kx}\,\mathrm{d}k, \quad t \geq 0, \tag{4.16}$$

https://doi.org/10.1017/jfm.2026.11138 Published online by Cambridge University Press

of (3.20) with initial data $\mathfrak{m}_0 \in \mathcal{S}(\mathbb{R})$. *We note now that if* $\lambda(k) = -ikc$ $(c \neq 0)$ *is a purely imaginary eigenvalue of* $\mathcal{M}(k)$ *with eigenvector* $\mathfrak{v}(k) \neq 0$, *then* e^{-ikct} *is an eigenvalue of* $e^{\mathcal{M}(k)\,t}$ *with eigenvector* $\mathfrak{v}(k)$. *Therefore, we see from (4.16) that the solution* $\mathfrak{m}(x,t)$ *of (3.20) acquires the form*

$$\frac{1}{2\pi}\int_{\mathbb{R}} \mathrm{e}^{\mathrm{i}k(x-ct)}\,\hat{\mathfrak{m}}_0(k)\,\mathrm{d}k. \tag{4.17}$$

This shows that a purely imaginary eigenvalue $\lambda(k) = -ikc$ *of* $\mathcal{M}(k)$ *corresponds to the fundamental oscillation mode* $\mathrm{e}^{\mathrm{i}k(x-ct)}\,\mathfrak{m}_0(k)$, *with frequency* $|k|/2\pi$, *and constant speed* c.

Searching now for solutions $\hat{\mathfrak{m}} = \hat{\mathfrak{m}}_0\,\mathrm{e}^{\mathrm{i}k(x-ct)}$ in (4.14) yields

$$(\mathcal{M}(k) + ikcI_6)\hat{\mathfrak{m}} = 0, \tag{4.18}$$

which implies $\det(\mathcal{M}(k) + ikcI_6) = 0$, since it is meaningful to require $\hat{\mathfrak{m}} \neq 0$. Since for $\lambda \in \mathbb{R}$ it holds that (and accounting for $A^0_{ij} := A^0_{ji}$ when $i > j$)

$$\begin{aligned}
&\det(\mathcal{M}(k) - \lambda I_6)\\
&= \lambda^6 - (b_1A^0_{11} + b_2A^0_{22} + b_3A^0_{33})\lambda^4\\
&\quad + [b_1b_2(A^0_{11}A^0_{22} - (A^0_{12})^2) + b_2b_3(A^0_{22}A^0_{33} - (A^0_{23})^2) + b_1b_3(A^0_{11}A^0_{33} - (A^0_{13})^2)]\lambda^2\\
&\quad - b_1b_2b_3\,\det(A^0_{i,j})_{i,j=\overline{1,3}},
\end{aligned} \tag{4.19}$$

we have that the wave speed c satisfies the equation

$$\begin{aligned}
&c^6 + \frac{b_1A^0_{11} + b_2A^0_{22} + b_3A^0_{33}}{k^2}c^4\\
&\quad + \frac{b_1b_2(A^0_{11}A^0_{22} - (A^0_{12})^2) + b_2b_3(A^0_{22}A^0_{33} - (A^0_{23})^2) + b_1b_3(A^0_{11}A^0_{33} - (A^0_{13})^2)}{k^4}c^2\\
&\quad + \frac{b_1b_2b_3\det(A^0_{ij})_{i,j=\overline{1,3}}}{k^6} = 0,
\end{aligned} \tag{4.20}$$

where $b_1 = -g\rho_1$, $b_2 = g(\rho_1 - \rho_2)$, $b_3 = g(\rho_2 - \rho_3)$. To ease further calculations, we find it useful to introduce the notation

$$\begin{aligned}
\Delta_1(k) &:= \rho_2\cosh(kh_3)\sinh(kh_b) + \rho_3\sinh(kh_3)\cosh(kh_b),\\
\Delta_2(k) &:= \rho_2\sinh(kh_3)\sinh(kh_b) + \rho_3\cosh(kh_3)\cosh(kh_b),\\
\Delta_3(k) &:= \rho_2\cosh(kh_3)\cosh(kh_1) + \rho_1\sinh(kh_1)\sinh(kh_3),\\
\Delta_4(k) &:= \rho_1\cosh(kh_3)\sinh(kh_1) + \rho_2\sinh(kh_3)\cosh(kh_1),\\
\Delta_5(k) &:= \rho_1\cosh(kh_1)\sinh(kh_3) + \rho_2\sinh(kh_1)\cosh(kh_3),
\end{aligned} \tag{4.21}$$

which entails

$$\Delta(k) = \rho_1\sinh(kh_1)\,\Delta_1(k) + \rho_2\cosh(kh_1)\,\Delta_2(k). \tag{4.22}$$

Setting also

$$\tilde{\Delta}(k) = \rho_3\cosh(kh_b)\,\Delta_3(k) + \rho_2\sinh(kh_b)\,\Delta_4(k), \tag{4.23}$$

https://doi.org/10.1017/jfm.2026.11138 Published online by Cambridge University Press

we have

$$M_{12} := A^0_{11}A^0_{22} - (A^0_{12})^2 = \frac{k^2\,\tilde{\Delta}(k)\,\Delta_1(k)\sinh(kh_1)}{\rho_1\,\Delta^2(k)},$$
$$M_{13} := A^0_{11}A^0_{33} - (A^0_{13})^2 = \frac{k^2\,\tilde{\Delta}(k)\,\Delta_5(k)\sinh(kh_b)}{\rho_1\,\Delta^2(k)}, \tag{4.24}$$
$$M_{23} := A^0_{22}A^0_{33} - (A^0_{23})^2 = \frac{k^2\,\tilde{\Delta}(k)\cosh(kh_1)\sinh(kh_b)\sinh(kh_3)}{\Delta^2(k)}.$$

The coefficients of (4.20) can now be written explicitly as

$$\begin{aligned}
a_4 &:= \frac{b_1A^0_{11} + b_2A^0_{22} + b_3A^0_{33}}{k^2}\\
&= \frac{g\big((\rho_2-\rho_1)(\rho_3-\rho_2)\sinh(kh_1)\sinh(kh_b)\sinh(kh_3) - \rho_2\rho_3\sinh(k(h_1+h_b+h_3))\big)}{k\,\Delta(k)},\\
a_2 &:= \frac{b_1b_2M_{12} + b_2b_3M_{23} + b_1b_3M_{13}}{k^4}\\
&= \frac{g^2\,\tilde{\Delta}(k)}{k^2\,\Delta^2(k)}\big((\rho_2-\rho_1)(\rho_3-\rho_2)\cosh(kh_1)\sinh(kh_b)\sinh(kh_3)\\
&\qquad + (\rho_2-\rho_1)\,\Delta_1\sinh(kh_1) + (\rho_3-\rho_2)\,\Delta_5\sinh(kh_b)\big),\\
a_0 &:= \frac{b_1b_2b_3\det(A^0_{ij})_{i,j=\overline{1,3}}}{k^6} = -\frac{g^3(\rho_2-\rho_1)(\rho_3-\rho_2)\sinh(kh_1)\sinh(kh_b)\sinh(kh_3)}{k^3\,\Delta(k)}.
\end{aligned} \tag{4.25}$$

4.2. *Short-wave limit*

The short-wave limit for the solutions of (4.20) can be obtained by using the asymptotics $\sinh(kh_i) \sim \pm(1/2)\exp(kh_i)$ and $\cosh(kh_i) \sim (1/2)\exp(kh_i)$ for $k \to \pm\infty$. Thus

$$a_4 \sim -\frac{g}{|k|}\left(1 + \frac{\rho_2-\rho_1}{\rho_2+\rho_1} + \frac{\rho_3-\rho_2}{\rho_3+\rho_2}\right), \tag{4.26}$$

$$a_2 \sim \frac{g^2}{k^2}\left(\frac{\rho_2-\rho_1}{\rho_2+\rho_1} + \frac{\rho_3-\rho_2}{\rho_3+\rho_2} + \frac{\rho_2-\rho_1}{\rho_2+\rho_1}\cdot\frac{\rho_3-\rho_2}{\rho_3+\rho_2}\right), \tag{4.27}$$

$$a_0 \sim -\frac{g^3}{|k|^3}\left(\frac{\rho_2-\rho_1}{\rho_2+\rho_1}\right)\left(\frac{\rho_3-\rho_2}{\rho_3+\rho_2}\right). \tag{4.28}$$

Thus the roots of (4.20) are real and given by the expressions

$$c_1^2 \sim \frac{g}{|k|}, \quad c_2^2 \sim \frac{g}{|k|}\left(\frac{\rho_2-\rho_1}{\rho_2+\rho_1}\right), \quad c_3^2 \sim \frac{g}{|k|}\left(\frac{\rho_3-\rho_2}{\rho_3+\rho_2}\right). \tag{4.29}$$

5. The long-wave limit

This section is devoted to an analysis of the dispersion relation giving the wave speed c in the long-wave limit $k \to 0$ for the case of three-layer flows. We note that the problem of several layers goes back to Stokes, and the general formula for the dispersion relation in the form of a determinant is provided in Greenhill (1886), where it is attributed to a Tripos exam question in Cambridge (1884), where Stokes has been Lucasian Professor. While the

https://doi.org/10.1017/jfm.2026.11138 Published online by Cambridge University Press

dispersion relation is a convoluted algebraic equation (whose degree is twice the number of layers), it exhibits interesting properties: it was shown by Benton (1954), Yih (1980) and Baines (1995), in the setting of steady flows of fixed mass flux, that all solutions of this equation (which, in fact, give the wave speeds) are real numbers. The central topics of this section are bounds for the roots of the dispersion relation as well as some approximate formulas for these roots together with a comparison between the solutions of the approximate formulas and the numerical solutions of the dispersion relation (5.1).

Utilising the findings in § 4 ,we infer that the equation for c corresponding to the long-wave limit ($k \to 0$) is

$$\begin{aligned} &c^6 - g(h_1+h_3+h_b)c^4 \\ &+ g^2\left[(\rho_2-\rho_1)\frac{h_1h_3}{\rho_2} + (\rho_3-\rho_2)\frac{h_3h_b}{\rho_3} + (\rho_3-\rho_1)\frac{h_1h_b}{\rho_3}\right]c^2 \\ &- g^3(\rho_2-\rho_1)(\rho_3-\rho_2)\frac{h_1h_3h_b}{\rho_2\rho_3} = 0, \end{aligned} \tag{5.1}$$

where we recall that the (mean) thickness of the upper layer is h_1, of the middle layer is h_3, and of the bottom layer is h_b. We also use the notation $h := h_3 + h_b$ and $H = h_1 + h = h_1 + h_3 + h_b$ (the total average depth of the fluid).

5.1. *Bounds for the roots of the dispersion relation*

To study (5.1) in greater detail, we denote $c^2 := X$, so we are led to consider the polynomial equation

$$\begin{aligned} &P(X) := X^3 - gHX^2 \\ &+ g^2\left[\rho_1(\rho_2-\rho_1)\frac{h_1h_3}{\rho_1\rho_2} + \rho_2(\rho_3-\rho_2)\frac{h_3h_b}{\rho_2\rho_3} + \rho_1(\rho_3-\rho_1)\frac{h_1h_b}{\rho_1\rho_3}\right]X \\ &- g^3\rho_1(\rho_2-\rho_1)(\rho_3-\rho_2)\frac{h_1h_3h_b}{\rho_1\rho_2\rho_3} = 0. \end{aligned} \tag{5.2}$$

The following result gives the interval where the roots of P lie.

PROPOSITION 5.1. *All the (real) roots of P lie in the interval* $(0, gH)$.

Proof. We readily note from above that the hypotheses $\rho_3 > \rho_2 > \rho_1$ and $h > h_3$ yield

$$P(0) < 0. \tag{5.3}$$

Furthermore, it is also easy to see that if $H_m \geq H = h + h_1$, then we have

$$\begin{aligned} P(gH_m) = g^3H_m^2(H_m - H) + g^3H_m\left[\rho_1(\rho_2-\rho_1)\frac{h_1h_3}{\rho_1\rho_2} + \rho_1(\rho_3-\rho_1)\frac{h_1h_b}{\rho_1\rho_3}\right] \\ + \frac{g^3(\rho_3-\rho_2)h_3h_b}{\rho_2\rho_3}\underbrace{(\rho_2H_m - (\rho_2-\rho_1)h_1)}_{\geq \rho_2h+\rho_1h_1} > 0. \end{aligned} \tag{5.4}$$

https://doi.org/10.1017/jfm.2026.11138 Published online by Cambridge University Press

Inequalities (5.3) and (5.4) yield that there is $X_1 \in (0,\, gH)$ such that $P(X_1) = 0$. Close inspection of the coefficients of P shows that $P(X) < 0$ for all $X \leq 0$. This implies that all the real roots of P lie in $(0,\, gH)$. □

Although explicit formulas are available for the roots of P, the intricacy of these formulas makes them difficult to use. Instead, using a general result of Prodanov (2022*a*,*b*), we provide bounds for the roots, defined in terms of the coefficients of P. First, we establish some notation. Let

$$\mathcal{A} := -gH, \tag{5.5}$$

$$\mathcal{B} := g^2\left[\frac{\rho_2-\rho_1}{\rho_2}h_1h_3 + \frac{\rho_3-\rho_2}{\rho_3}h_3h_b + \frac{\rho_3-\rho_1}{\rho_3}h_1h_b\right], \tag{5.6}$$

$$\mathcal{C} := -g^3(\rho_2-\rho_1)(\rho_3-\rho_2)\frac{h_1h_3h_b}{\rho_2\rho_3} \tag{5.7}$$

be the coefficients of the polynomial from (5.2).

The locations of the three roots of the polynomial $P(X)$ depend (cf. Prodanov 2022*a*,*b*) on the ratio $\mathcal{B}/\mathcal{A}^2$, which will be analysed in the sequel. For a fixed value of $\mathcal{A}$ (i.e. for a fixed total depth H), the maximum of $\mathcal{B}$ can be found, for example, from the Lagrangian function

$$L(h_1, h_3, h_b, \lambda) = \mathcal{B}(h_1, h_3, h_b) - \lambda(h_1 + h_3 + h_b - H). \tag{5.8}$$

The maximal value of $\mathcal{B}$ is

$$\mathcal{B}_{max} = \frac{\rho_2(\rho_3-\rho_1)g^2H^2}{\rho_2^2 + (3\rho_3-\rho_1)\rho_2 + \rho_3\rho_1} = \frac{\nu_2(1-\nu_1)}{\nu_2^2 + (3-\nu_1)\nu_2 + \nu_1}\mathcal{A}^2 \tag{5.9}$$

(where $\nu_1 = \rho_1/\rho_3 < 1$ and $\nu_2 = \rho_2/\rho_3 < 1$), attained for

$$h_1^0 = \frac{(\rho_2+\rho_3)\rho_2}{\rho_2^2 + (3\rho_3-\rho_1)\rho_2 + \rho_3\rho_1}H, \tag{5.10}$$

$$h_3^0 = \frac{(\rho_3-\rho_1)\rho_2}{\rho_2^2 + (3\rho_3-\rho_1)\rho_2 + \rho_3\rho_1}H, \tag{5.11}$$

$$h_b^0 = \frac{(\rho_1+\rho_2)\rho_3}{\rho_2^2 + (3\rho_3-\rho_1)\rho_2 + \rho_3\rho_1}H. \tag{5.12}$$

It is easy to check that

$$\frac{\nu_2(1-\nu_1)}{\nu_2^2 + (3-\nu_1)\nu_2 + \nu_1} < \frac{1}{3}, \tag{5.13}$$

thus we always have $0 < \mathcal{B} < (1/3)\mathcal{A}^2$. In Prodanov (2022*a*,*b*), three possible scenarios for the ratio $\mathcal{B}/\mathcal{A}^2$ can occur:

$$0 < \mathcal{B} < \frac{2}{9}\mathcal{A}^2, \tag{5.14}$$

$$\frac{2}{9}\mathcal{A}^2 < \mathcal{B} < \frac{1}{4}\mathcal{A}^2, \tag{5.15}$$

$$\frac{1}{4}\mathcal{A}^2 < \mathcal{B} < \frac{1}{3}\mathcal{A}^2. \tag{5.16}$$

https://doi.org/10.1017/jfm.2026.11138 Published online by Cambridge University Press

In each of the above scenarios, bounds detailing the locations of the three positive roots of $P(X)$ are available; cf. (5.22) below. Before passing to a discussion on these bounds, we examine the term on the left-hand side of (5.13), so we identify some conditions for the fulfilment of (5.14), (5.15) and (5.16). These conditions are given in terms of the ratio between the density of the top layer and suitable linear combinations of the densities of the other layers as follows:

$$\text{(i) } 0 < \mathcal{B} < \frac{2}{9}\mathcal{A}^2 \quad \text{when} \quad \nu_1 > \frac{\nu_2(3-2\nu_2)}{7\nu_2+2}, \quad \text{i.e.} \quad \rho_1 > \rho_U = \frac{3\rho_3 - 2\rho_2}{7\rho_2 + 2\rho_3}\rho_2; \tag{5.17}$$

$$\text{(ii) } 0 < \mathcal{B} < \frac{1}{4}\mathcal{A}^2 \quad \text{when} \quad \nu_1 > \frac{\nu_2(1-\nu_2)}{3\nu_2+1}, \quad \text{i.e.} \quad \rho_1 > \rho_L = \frac{\rho_3 - \rho_2}{3\rho_2 + \rho_3}\rho_2. \tag{5.18}$$

Of course, we always have $\rho_U > \rho_L$. The above conditions in terms of the densities are only sufficient conditions. Unfortunately, there is no simple criterion (in terms of densities) that discriminates between (5.14), (5.15) and (5.16). For example, a necessary (but not sufficient) condition to have the situation in (5.16) is

$$\rho_1 < \rho_L = \frac{\rho_3 - \rho_2}{3\rho_2 + \rho_3}\rho_2. \tag{5.19}$$

In most practical-relevant situations, the relative differences in densities are relatively small. It can be shown that this assumption leads to the situation in (5.14). More precisely, assuming that

$$\frac{\rho_2 - \rho_1}{\rho_2} < \frac{4}{9}, \quad \frac{\rho_3 - \rho_2}{\rho_3} < \frac{4}{9}, \quad \frac{\rho_3 - \rho_1}{\rho_3} < \frac{4}{9}, \tag{5.20}$$

and using the Cauchy–Schwartz inequality, we infer from (5.6) that

$$\mathcal{B} < \frac{4}{9}g^2(h_1 h + h_3(h - h_3)) < \frac{4}{9}g^2\left(h_1 h + \frac{h^2}{4}\right) < \frac{4}{9}g^2\frac{(h+h_1)^2}{2} = \frac{2}{9}\mathcal{A}^2. \tag{5.21}$$

Therefore, (5.20) is another sufficient condition that leads to the case (5.14). In practical applications, the internal waves occur between layers of one type of liquid (or very similar liquids) with slightly different properties (and densities), thus the condition (5.20) covers a wide range of practically possible situations.

According to Prodanov (2022*a*,*b*), when $\mathcal{A} < 0$ for the three real roots of $P(X)$, denoted by $0 < X_3 \le X_2 \le X_1$, in the case (5.14) the following bounds are valid:

$$\begin{aligned} 0 < -\mathcal{C} &\le -\mathcal{C}_2, \\ -\frac{\mathcal{C}}{\mathcal{B}} &\le X_3 \le \mu_2, \\ \mu_2 &\le X_2 \le \lambda_2, \\ \lambda_1 &\le X_1 \le \sigma_2, \end{aligned} \tag{5.22}$$

https://doi.org/10.1017/jfm.2026.11138 Published online by Cambridge University Press

where the following notations are used:

$$\mathcal{C}_1 := -\frac{2\mathcal{A}^3}{27} + \frac{\mathcal{A}\mathcal{B}}{3} + \frac{2}{27}\sqrt{(\mathcal{A}^2 - 3\mathcal{B})^3}, \quad \mathcal{C}_2 := -\frac{2\mathcal{A}^3}{27} + \frac{\mathcal{A}\mathcal{B}}{3} - \frac{2}{27}\sqrt{(\mathcal{A}^2 - 3\mathcal{B})^3},$$
$$\lambda_1 := -\frac{\mathcal{A}}{2} + \sqrt{\frac{\mathcal{A}^2}{4} - \mathcal{B}}, \quad \lambda_2 := -\frac{\mathcal{A}}{2} - \sqrt{\frac{\mathcal{A}^2}{4} - \mathcal{B}},$$
$$\mu_1 := -\frac{\mathcal{A}}{3} + \frac{\sqrt{3}}{3}\sqrt{\frac{\mathcal{A}^2}{3} - \mathcal{B}}, \quad \mu_2 := -\frac{\mathcal{A}}{3} - \frac{\sqrt{3}}{3}\sqrt{\frac{\mathcal{A}^2}{3} - \mathcal{B}}, \tag{5.23}$$

and

$$\sigma_1 := -\frac{\mathcal{A}}{3} - 2\frac{\sqrt{3}}{3}\sqrt{\frac{\mathcal{A}^2}{3} - \mathcal{B}}, \quad \sigma_2 := -\frac{\mathcal{A}}{3} + 2\frac{\sqrt{3}}{3}\sqrt{\frac{\mathcal{A}^2}{3} - \mathcal{B}}. \tag{5.24}$$

5.2. *Approximate solutions for the wave speeds*

We provide here some further insights resulting from (5.1). More precisely, we take into account several propagation regimes defined by the mutual relations existing between monomials in (5.1). We distinguish the following cases.

(i) If a_2c^2 and c_0 are much smaller than c^6 and a_4c^4, then the approximate equation that we obtain has the roots $\pm\sqrt{gH}$. However, from estimates (5.22) for the largest root, we observe that if $\mathcal{B}/\mathcal{A}^2 \ll 1$, then

$$\sigma_2 = |\mathcal{A}|\left[1 - \frac{\mathcal{B}}{\mathcal{A}^2} + \mathcal{O}\left(\left(\frac{\mathcal{B}}{\mathcal{A}^2}\right)^2\right)\right], \tag{5.25}$$

$$\lambda_1 = |\mathcal{A}|\left[1 - \frac{\mathcal{B}}{\mathcal{A}^2} + \mathcal{O}\left(\left(\frac{\mathcal{B}}{\mathcal{A}^2}\right)^2\right)\right], \tag{5.26}$$

and the next correction to the approximate expression $X_1 \approx gH$ is

$$X_1 \approx |\mathcal{A}| - \frac{\mathcal{B}}{|\mathcal{A}|} = gH - \frac{g}{H}\left[\frac{\rho_2 - \rho_1}{\rho_2}h_1h_3 + \frac{\rho_3 - \rho_2}{\rho_3}h_3h_b + \frac{\rho_3 - \rho_1}{\rho_3}h_1h_b\right]. \tag{5.27}$$

Thus the propagation speed on the surface is approximately

$$c_{1,a} = \pm\sqrt{gH - \frac{g}{H}\left[\frac{\rho_2 - \rho_1}{\rho_2}h_1h_3 + \frac{\rho_3 - \rho_2}{\rho_3}h_3h_b + \frac{\rho_3 - \rho_1}{\rho_3}h_1h_b\right]}. \tag{5.28}$$

(ii) The dominant terms are a_4c^4 and a_2c^2. Indeed, from (5.22), for X_2 if $\mathcal{B}/\mathcal{A}^2 \ll 1$, then we have

$$\mu_2 = \frac{\mathcal{B}}{2\,|\mathcal{A}|} + |\mathcal{A}|\,\mathcal{O}\left(\left(\frac{\mathcal{B}}{\mathcal{A}^2}\right)^2\right), \tag{5.29}$$

$$\lambda_2 = \frac{\mathcal{B}}{|\mathcal{A}|} + |\mathcal{A}|\,\mathcal{O}\left(\left(\frac{\mathcal{B}}{\mathcal{A}^2}\right)^2\right), \tag{5.30}$$

therefore X_2 is of order $\mathcal{B}/|\mathcal{A}| \ll X_1$. Moreover, again from (5.22), $(|\mathcal{C}|/\mathcal{B}) < \mu_2 \approx \mathcal{B}/2|\mathcal{A}|$, thus $\mathcal{B}^2 > 2\,|\mathcal{A}\mathcal{C}|$. This justifies the further assumption $\mathcal{B}^2 \gg |\mathcal{A}\mathcal{C}|$, under

https://doi.org/10.1017/jfm.2026.11138 Published online by Cambridge University Press

No.	ρ_1	ρ_2	ρ_3	h_1	h_3	h_b	$c_{1,a}/\sqrt{gH}$	$c_{2,a}/\sqrt{gH}$	$c_{3,a}/\sqrt{gH}$	$c_i/\sqrt{gH}$
1	1000	1010	1020	200	100	300	0.9976	0.0680	0.0241	0.9976, 0.0630, 0.0261
2	1000	1020	1100	10	100	3000	0.9987	0.0504	0.0075	0.9987, 0.0499, 0.0076
3	1005	1016	1027	600	100	3000	0.9984	0.0557	0.0115	0.9984, 0.0545, 0.0118
4	997	999	1000	6	2	20	0.9997	0.0233	0.00636	0.9997, 0.0223, 0.00664
5	997	999	1000	10	20	50	0.9998	0.0212	0.00929	0.9998, 0.0184, 0.01078
6	650	1500	5500	0.02	0.05	0.03	0.8839	0.4676	0.2378	0.8487, 0.4346, 0.3015
7	620	1900	5900	0.02	0.05	0.03	0.8816	0.4720	0.2480	0.8458, 0.4188, 0.3304

Table 1. The approximate and exact wave speeds for some values of the parameters. Rows 1 and 2 correspond to internal waves, row 3 refers to equatorial internal waves, rows 4 and 5 pertain to three-layer lakes, and rows 6 and 7 refer to laboratory experiments. The dimensionalities of all quantities are given in the International System of Units (SI), $g = 9.81\ \mathrm{m\,s^{-2}}$. All velocities are given in non-dimensional units by division by $\sqrt{gH}$. The quantities c_i are the positive roots of (5.1).

which it can be seen that when $c^2 = X_2$, the dominant terms in the equation are a_4c^4 and a_2c^2. Then the solution of the approximate equation gives $c_{2,a}^2 = \mathcal{B}/|\mathcal{A}|$ or

$$c_{2,a} = \pm\sqrt{\frac{g}{H}\left[\frac{\rho_2-\rho_1}{\rho_2}h_1h_3 + \frac{\rho_3-\rho_2}{\rho_3}h_3h_b + \frac{\rho_3-\rho_1}{\rho_3}h_1h_b\right]}. \tag{5.31}$$

(iii) The dominant terms are a_2c^2 and a_0. From Viète formulas, we have

$$X_1X_2X_3 = -\mathcal{C} = |\mathcal{C}|. \tag{5.32}$$

In the leading order, $X_1 = |A|$ and $X_2 = \mathcal{B}/|\mathcal{A}|$, therefore $X_3 = |\mathcal{C}/\mathcal{B}|$, thus

$$c_{3,a} = \pm\sqrt{\frac{g(\rho_3-\rho_2)(\rho_2-\rho_1)h_1h_bh_3}{h_1h_b\rho_2(\rho_3-\rho_1) + h_bh_3\rho_2(\rho_3-\rho_2) + h_1h_3\rho_3(\rho_2-\rho_1)}}. \tag{5.33}$$

In these derivations, we made the assumptions $\mathcal{B}/\mathcal{A}^2 \ll 1$ and $\mathcal{B}^2 \gg |\mathcal{AC}|$, which are compatible with the inequalities of (5.14), and of course with all kind of realistic physical data. Therefore, it is expected that the approximate formulas perform best in this case. Nevertheless, the results in table 1 show that (5.28), (5.31) and (5.33) perform quite well also in (5.15) and (5.16).

REMARK 5.2. *The two-layer limit case $\rho_3 = \rho_2$, with depths h_1 and h in (5.28) leads to*

$$c_{1,a}^* = \pm\sqrt{g(h_1+h)\left(1 - \frac{h_1h}{(h_1+h)^2}\frac{\rho_2-\rho_1}{\rho_2}\right)}. \tag{5.34}$$

This appears also in e.g. Craig et al. (2005) and Kodaira et al. (2016).

REMARK 5.3. *The two-layer limit case $\rho_3 = \rho_2$, with depths h_1 and h in (5.31), leads to the well-known formula for the phase speed of an internal wave, which is related to the so-called Brunt–Väisälä frequency,*

$$c_{2,a}^* = \pm\sqrt{\frac{g(\rho_2-\rho_1)hh_1}{\rho_2(h+h_1)}}. \tag{5.35}$$

https://doi.org/10.1017/jfm.2026.11138 Published online by Cambridge University Press

As a matter of fact, the precise formula for two layers in the rigid lid approximation is formula (4.5) of Craig et al. (2005), but because in the ocean the two densities are very close ($\rho_1 \approx \rho_2$), in many situations (5.35) is used instead (Massel 2015; Kodaira et al. 2016).

The propagation speed (5.31) is associated with the disturbance described by η_2 because the internal wave formed at this interface usually has a significant amplitude moving with the mentioned speed. Clearly, $\sqrt{gH}$ is the speed of the surface waves (over the total depth H) which due to the influence of the interfaces is modified to (5.28), while (5.33) is the speed of internal waves, observable at the interface $y = \eta_3$. In general, waves with all possible speeds have their traces on the surface and on both interfaces. However, their amplitudes can be of quite different magnitudes.

Table 1 displays a comparison between the solutions of the approximate formulas above and the (positive) numerical solutions of (5.1). It is remarkable that the approximate formulas (5.28)–(5.33) give a very good approximation (for a range of physically feasible values of the parameters) to the actual solutions of (5.1). Rows 1–6 of table 1 correspond to (5.14), and the approximation formulas provide very good approximations. Row 7 illustrates (5.15). It does not seem that there are any real-life examples satisfying case (5.16). The cases (5.15) and (5.16) exhibit very large differences in the densities, and are not realistic in an oceanographic context. The approximation formulas work less well in the examples that exhibit large density contrasts, but nevertheless the approximate values are very good as a guide to the locations of the exact ones.

The first example in table 1 reflects typical parameter values for interfacial ocean internal waves. The next example (shown as no. 2 in table 1) concerns oceanographic and limnological systems, where stratified water columns are common due to variations in temperature, salinity and pressure. A three-layer structure with densities approximately 1000, 1020 and 1100 kg m^{-3}, and respective thicknesses 10, 100 and 3000 m, can be justified by combining observations from coastal, open ocean and hypersaline environments; cf. https://oceanexplorer.noaa.gov/technology/ctd/ctd.html, https://www.bodc.ac.uk/data/bodc_database/ctd/, https://podaac.jpl.nasa.gov/dataset/OMG_L2_CTD.

The third example (no. 3 in table 1) is with parameter values, typical for the internal equatorial waves in the Pacific Ocean; see e.g. Constantin & Ivanov (2019). The total depth of the Pacific Ocean is approximately 4000 m on average, and the upper layer is several hundred metres deep. We note that standard seawater density rarely exceeds 1050 kg m^{-3}.

The next two examples (nos 4 and 5 in table 1) of a three-layer system concern temperate lakes, in which – particularly during the summer stratification period – the water column consistently organises into three distinct layers: the epilimnion, metalimnion and hypolimnion. The epilimnion, which typically extends from the surface to depths of 5–20 m, is a warm, well-mixed layer influenced by wind and solar heating. Beneath it lies the metalimnion, or thermocline, a transition zone several metres thick, where temperature and density change rapidly with depth, effectively inhibiting vertical mixing. The hypolimnion, the coldest and densest layer, lies below the thermocline and remains largely isolated from surface influences, often becoming oxygen-depleted over time because of biological activity and lack of mixing. This three-layer structure is not just a convenient simplification, but a physically necessary framework that accurately captures the thermal, chemical and biological dynamics of stratified lakes. Unlike oceanographic systems, where stratification is governed by both temperature and salinity over much greater depths, lake stratification is shallow, thermally driven and seasonally reversible, reflecting the unique density behaviour of freshwater and the limited depth of most inland water bodies (cf. Huttula 2012).

https://doi.org/10.1017/jfm.2026.11138 Published online by Cambridge University Press

To investigate flow behaviour in sharply stratified systems, we consider (in rows 6 and 7 of table 1) a three-layer fluid column with engineered density contrasts that far exceed those found in natural oceanographic environments (see National Institute of Standards and Technology, US Department of Commerce, NIST Chemistry WebBook, SRD 69). Unlike ocean stratification, which typically involves density differences of only 1–3 % due to temperature and salinity gradients, this system spans nearly an order of magnitude in density, using immiscible or semi-miscible fluids to maintain stable, well-defined interfaces.

The top layer typically consists of light hydrocarbons such as pentane or hexane. These fluids have densities in the range 600–700 kg m^{-3} and form a buoyant, sharply defined upper boundary. In experimental set-ups, this layer is often kept relatively thin, with height approximately 1–2 cm, to minimise mixing and maintain interface clarity.

The middle layer is composed of dense aqueous solutions, such as $ZnCl_2$ brines or glycerol–water mixtures, with densities in the range 1000–2200 kg m^{-3}. This layer serves as a transitional buffer and is typically the thickest, with heights 3–5 cm, allowing for stable stratification and tunable flow dynamics. Its density can be adjusted to fine-tune the separation between the top and bottom layers.

The bottom layer features ultra-dense fluids such as perfluorodecalin, or liquid metals such as gallium alloys, which can reach densities 6400 kg m^{-3}. This layer is usually 1–3 cm thick and provides a heavy, immiscible foundation that anchors the system and prevents upward mixing.

6. The limit to two layers with a free surface

We show here that the dispersion relation for the two-layer case, known from previous works of Lamb (1932) and Craig *et al.* (2005), follows from considerations about the three-layer setting, as a particular case of (4.20). In this case, we set $\rho_3 = \rho_2$. Then taking into account (4.9) and (4.10), we have

$$\begin{aligned} A^0_{11} &= k\frac{\tanh(kh)\coth(kh_1)+\rho_2/\rho_1}{\rho_2\coth(kh_1)+\rho_1\tanh(kh)},\\ A^0_{12} &= k\frac{\tanh(kh)}{\sinh(kh_1)\big(\rho_2\coth(kh_1)+\rho_1\tanh(kh)\big)},\\ A^0_{22} &= k\frac{\tanh(kh)\coth(kh_1)}{\rho_2\coth(kh_1)+\rho_1\tanh(kh)}. \end{aligned} \tag{6.1}$$

Therefore, expanding the determinant of the matrix $\mathcal{M}(k)-\lambda I_6$ by row three, we obtain

$$\det(\mathcal{M}(k)-\lambda I_6) = \lambda^2\big[\lambda^4-(b_1A^0_{11}+b_2A^0_{22})\lambda^2+b_1b_2\big(A^0_{11}A^0_{22}-(A^0_{12})^2\big)\big]. \tag{6.2}$$

Further, we find from (6.1) that

$$b_1A^0_{11}+b_2A^0_{22} = -g\rho_2k\frac{1+\tanh(kh)\coth(kh_1)}{\rho_2\coth(kh_1)+\rho_1\tanh(kh)}, \tag{6.3a}$$

$$b_1b_2\big(A^0_{11}A^0_{22}-(A^0_{12})^2\big) = \frac{g^2(\rho_2-\rho_1)k^2\tanh(kh_1)\tanh(kh)}{\rho_2+\rho_1\tanh(kh_1)\tanh(kh)}. \tag{6.3b}$$

Proceeding as before, i.e. searching for solutions $\hat{u}=\hat{u}_0\,\mathrm{e}^{\mathrm{i}k(x-ct)}$ in (4.14) and denoting $\omega(k) := ck$, which is the spatial frequency of the wave solution, we notice from (6.2) and

https://doi.org/10.1017/jfm.2026.11138 Published online by Cambridge University Press

(6.3) that ω satisfies the equation

$$\omega^4 - g\rho_2 k\frac{1+\tanh(kh)\coth(kh_1)}{\rho_2\coth(kh_1)+\rho_1\tanh(kh)}\omega^2 + \frac{g^2(\rho_2-\rho_1)k^2\tanh(kh_1)\tanh(kh)}{(\rho_2+\rho_1\tanh(kh_1)\tanh(kh))} = 0, \tag{6.4}$$

i.e. we recover the equation obtained by Craig *et al.* (2005) with Hamiltonian methods. This equation apparently goes back to Lamb (1932), where the problem of 'superimposed liquids' is solved.

REMARK 6.1. *Denoting $\omega^2 := Y$, we observe that Y satisfies a second-degree algebraic equation whose discriminant is $\Delta = (b_1A_{11} - b_2A_{22})^2 + 4b_1b_2(A_{12})^2 > 0$, which shows that this equation has two real roots, called Y_1, Y_2. Since*

$$Y_1 + Y_2 = g\rho_2 k\frac{1+\tanh(kh)\coth(kh_1)}{\rho_2\coth(kh_1)+\rho_1\tanh(kh)} > 0, \tag{6.5a}$$

$$Y_1 \cdot Y_2 = \frac{g^2(\rho_2-\rho_1)k^2\tanh(kh_1)\tanh(kh)}{\rho_2+\rho_1\tanh(kh_1)\tanh(kh)} > 0, \tag{6.5b}$$

we infer that Y_1 and Y_2 are positive, i.e. (6.4) has four real roots.

7. The rigid lid model

In this section, we discuss the rigid lid model, which corresponds to a flat surface $\eta_1(x,t) \equiv 0$. The difference from the model with a non-trivial free surface is that for the domain Ω_1 of the upper layer, we have a single DN operator, namely $G_1(\eta_2)$.

7.1. *The DN operators and evolution equations*

We use the techniques developed in the previous sections and repeat the same steps. The Hamiltonian formulation can be established in this case as well; however, we are going to employ only techniques related to the DN operators. For the middle and lower layers, we have the DN operators (3.22) and (3.23). The DN operator for the upper layer is as in (2.12) of Craig *et al.* (2005) and is defined as

$$\left(\frac{\partial\varphi_1}{\partial(-\boldsymbol{n}_2)}\right)_{s_2}\sqrt{1+\eta_{2,x}^2} = -\boldsymbol{n}_2\cdot(\nabla\varphi_1)_{s_2} \equiv -G_1(\eta_2)(\varphi_1)_{s_2}. \tag{7.1}$$

More details are provided in (A.10) of Craig *et al.* (2005), e.g.

$$G_1(\eta_2) = \sum_{l=0}^{\infty} G_1^{(l)}(\eta_2), \tag{7.2}$$

$$G_1^{(0)} = D\tanh(h_1D), \quad G_1^{(1)} = -D\eta_2(x)\,D + G_1^{(0)}\,\eta_2(x)\,G_1^{(0)} + \cdots. \tag{7.3}$$

Then obviously

$$\eta_{2,t} = -G_1(\eta_2)(\varphi_1)_{s_2} = \Gamma_{11}(\varphi_2)_{s_2} + \Gamma_{12}(\varphi_2)_{s_3}, \tag{7.4}$$

and as in (3.27), we obtain

$$\eta_{3,t} = G(\eta_3)(\varphi_3)_{s_3} = -[\Gamma_{21}(\varphi_2)_{s_2} + \Gamma_{22}(\varphi_2)_{s_3}]. \tag{7.5}$$

Equations (7.4) and (7.5) together with

$$\xi_2 := \rho_2(\varphi_2)_{s_2} - \rho_1(\varphi_1)_{s_2}, \quad \xi_3 := \rho_3(\varphi_3)_{s_3} - \rho_2(\varphi_2)_{s_3} \tag{7.6}$$

https://doi.org/10.1017/jfm.2026.11138 Published online by Cambridge University Press

can be solved for $(\varphi_1)_{s_2}$, $(\varphi_2)_{s_2}$, $(\varphi_2)_{s_3}$ and $(\varphi_3)_{s_3}$ in terms of ξ_2, ξ_3 and the corresponding DN operators (that depend on η_2 and η_3). We obtain the following expressions (different from those in (3.35) and (3.36)):

$$(\varphi_2)_{s_2} = B^{-1}\left[\rho_1 G\xi_3 + (\rho_3\Gamma_{22} + \rho_2 G)\Gamma_{12}^{-1}G_1\xi_2\right] =: \Phi_2^2(\eta_i, \xi_i), \tag{7.7}$$

$$(\varphi_2)_{s_3} = -(B^*)^{-1}\left[\rho_3 G_1\xi_2 + (\rho_1\Gamma_{11} + \rho_2 G_1)\Gamma_{21}^{-1}G\xi_3\right] =: \Phi_3^2(\eta_i, \xi_i), \tag{7.8}$$

where

$$B = (\rho_3\Gamma_{22} + \rho_2 G)\Gamma_{12}^{-1}(\rho_2 G_1 + \rho_1\Gamma_{11}) - \rho_1\rho_3\Gamma_{21}. \tag{7.9}$$

This allows to express (7.4) and (7.5) in the form

$$\eta_{2,t} = A_{22}\xi_2 + A_{23}\xi_3, \tag{7.10}$$

$$\eta_{3,t} = A_{32}\xi_2 + A_{33}\xi_3, \tag{7.11}$$

where

$$A_{22} = -\rho_3\Gamma_{12}(B^*)^{-1}G_1 + \Gamma_{11}B^{-1}(\rho_3\Gamma_{22} + \rho_2 G)\Gamma_{12}^{-1}G_1, \tag{7.12}$$

$$A_{23} = \rho_1\Gamma_{11}B^{-1}G - \Gamma_{12}(B^*)^{-1}(\rho_1\Gamma_{11} + \rho_2 G_1)\Gamma_{21}^{-1}G, \tag{7.13}$$

$$A_{32} = \rho_3\Gamma_{22}(B^*)^{-1}G_1 - \Gamma_{21}B^{-1}(\rho_3\Gamma_{22} + \rho_2 G)\Gamma_{12}^{-1}G_1, \tag{7.14}$$

$$A_{33} = -\rho_1\Gamma_{21}B^{-1}G + \Gamma_{22}(B^*)^{-1}(\rho_1\Gamma_{11} + \rho_2 G_1)\Gamma_{21}^{-1}G \tag{7.15}$$

are operators that depend only on η_2 and η_3. These operators, of course, are not the same as those in (3.38). Thus defining

$$F_2(\eta_i, \xi_i) := A_{22}\xi_2 + A_{23}\xi_3, \quad F_3(\eta_i, \xi_i) := A_{32}\xi_2 + A_{33}\xi_3, \quad i = 2, 3, \tag{7.16}$$

we have the nonlinear dynamics for η_2 and η_3 from (7.4) in the form

$$\eta_{2,t} = F_2(\eta_i, \xi_i), \quad \eta_{3,t} = F_3(\eta_i, \xi_i), \tag{7.17}$$

and also

$$(\varphi_1)_{s_2} = -G_1^{-1}\eta_{2,t} = -G_1(\eta_2)^{-1}F_2(\eta_i, \xi_i) =: \Phi_2^1(\eta_i, \xi_i), \tag{7.18}$$

$$(\varphi_3)_{s_3} = G^{-1}\eta_{3,t} = G(\eta_3)^{-1}F_3(\eta_i, \xi_i) =: \Phi^3(\eta_i, \xi_i). \tag{7.19}$$

The time evolution of ξ_2 and ξ_3 is given by (3.53) and (3.55) as

$$\xi_{2,t} + \frac{\rho_2(\Phi_{2,x}^2)^2 - \rho_1(\Phi_{2,x}^1)^2 - 2F_2\xi_{2,x}\eta_{2,x} + (\rho_1 - \rho_2)F_2^2}{2(1+\eta_{2,x}^2)} + (\rho_2 - \rho_1)g\eta_2 = 0, \tag{7.20}$$

$$\xi_{3,t} + \frac{\rho_3(\Phi_x^3)^2 - \rho_2(\Phi_{3,x}^2)^2 - 2F_3\xi_{3,x}\eta_{3,x} + (\rho_2 - \rho_3)F_3^2}{2(1+\eta_{3,x}^2)} + (\rho_3 - \rho_2)g\eta_3 = 0, \tag{7.21}$$

with the new definitions of F_2, F_3 in (7.16), and the quantities in (7.7), (7.8), (7.18) and (7.19).

Thus we have the full nonlinear system of the time evolution in terms of DN operators given by (7.17), (7.20) and (7.21). We will illustrate how this system produces model equations in different propagation regimes.

https://doi.org/10.1017/jfm.2026.11138 Published online by Cambridge University Press

7.2. *Leading-order linear approximation and dispersion relation*

In the leading-order approximation, we are using the DN operators from (7.3), (4.8) and (4.7) to obtain

$$A^0_{22}(k) = \frac{k[\rho_2 \cosh(kh_3)\sinh(kh_b) + \rho_3 \sinh(kh_3)\cosh(kh_b)]\sinh(kh_1)}{\boldsymbol{D}(k)}, \tag{7.22}$$

$$A^0_{23}(k) = A^0_{32}(k) = \frac{k\rho_2 \sinh(kh_b)\sinh(kh_1)}{\boldsymbol{D}(k)}, \tag{7.23}$$

$$A^0_{33}(k) = \frac{k[\rho_1 \cosh(kh_1)\sinh(kh_3) + \rho_2 \cosh(kh_3)\sinh(kh_1)]\sinh(kh_b)}{\boldsymbol{D}(k)}, \tag{7.24}$$

where

$$\begin{aligned}\boldsymbol{D}(k) = {}& \rho_2\Big(\rho_3 \cosh(kh_3)\cosh(kh_b) + \rho_2 \sinh(kh_3)\sinh(kh_b)\Big)\sinh(kh_1) \\ & + \rho_1\Big(\rho_2 \cosh(kh_3)\sinh(kh_b) + \rho_3 \sinh(kh_3)\cosh(kh_b)\Big)\cosh(kh_1).\end{aligned} \tag{7.25}$$

Note that for $k \neq 0$, the sign of $\boldsymbol{D}(k)$ coincides with the sign of k, thus $\boldsymbol{D}(k) \neq 0$. The equations for ξ_i are as in (4.13), and the linearised equations in the leading-order approximation therefore are

$$\eta_{2,t} = A^0_{22}(D)\,\xi_2 + A^0_{23}(D)\,\xi_3, \tag{7.26}$$

$$\eta_{3,t} = A^0_{32}(D)\,\xi_2 + A^0_{33}(D)\,\xi_3, \tag{7.27}$$

$$\xi_{2,t} = -g(\rho_2 - \rho_1)\eta_2, \tag{7.28}$$

$$\xi_{3,t} = -g(\rho_3 - \rho_2)\eta_3. \tag{7.29}$$

The analogue of the matrix $\mathcal{M}$ in (4.14) is now

$$\mathcal{M}(k) = \begin{pmatrix} 0 & 0 & A^0_{22}(k) & A^0_{23}(k) \\ 0 & 0 & A^0_{23}(k) & A^0_{33}(k) \\ g(\rho_1 - \rho_2) & 0 & 0 & 0 \\ 0 & g(\rho_2 - \rho_3) & 0 & 0 \end{pmatrix}. \tag{7.30}$$

The characteristic equation $\det(\mathcal{M}(k) + ikcI_4) = 0$ leads to the following bi-quadratic equation for the propagation speeds c:

$$c^4 + a_2c^2 + a_0 = 0, \tag{7.31}$$

$$a_2 = -\frac{g(A^0_{22}(\rho_2 - \rho_1) + A^0_{33}(\rho_3 - \rho_2))}{k^2} = -\frac{g\,\boldsymbol{D}_1(k)}{k\,\boldsymbol{D}(k)}, \tag{7.32}$$

$$\begin{aligned} a_0 &= \frac{g^2(\rho_3 - \rho_2)(\rho_2 - \rho_1)(A^0_{22}A^0_{33} - (A^0_{23})^2)}{k^4} \\ &= \frac{g^2(\rho_3 - \rho_2)(\rho_2 - \rho_1)\sinh(kh_1)\sinh(kh_3)\sinh(kh_b)}{k^2\,\boldsymbol{D}(k)}, \end{aligned} \tag{7.33}$$

where

$$\begin{aligned}\boldsymbol{D}_1(k) = {}& [\rho_2(\rho_3 - \rho_1)\cosh(kh_3)\sinh(kh_b) \\ & + \rho_3(\rho_2 - \rho_1)\sinh(kh_3)\cosh(kh_b)]\sinh(kh_1) \\ & + \rho_1(\rho_3 - \rho_2)\cosh(kh_1)\sinh(kh_3)\sinh(kh_b).\end{aligned} \tag{7.34}$$

https://doi.org/10.1017/jfm.2026.11138 Published online by Cambridge University Press

7.3. *Short-wave limit*

The short-wave limit for the solutions of (7.31) can be obtained in a similar way by the asymptotics $\sinh(kh_i) \sim \pm(1/2)\exp(kh_i)$ and $\cosh(kh_i) \sim (1/2)\exp(kh_i)$ for $k \to \pm\infty$. Thus

$$a_2 \sim -\frac{g}{|k|}\left(\frac{\rho_2-\rho_1}{\rho_2+\rho_1}+\frac{\rho_3-\rho_2}{\rho_3+\rho_2}\right), \tag{7.35}$$

$$a_0 \sim \frac{g^2}{k^2}\left(\frac{\rho_2-\rho_1}{\rho_2+\rho_1}\right)\left(\frac{\rho_3-\rho_2}{\rho_3+\rho_2}\right). \tag{7.36}$$

The roots of (7.31) are real as well, and coincide with the two already known values in (4.29):

$$c_1^2 \sim \frac{g}{|k|}\left(\frac{\rho_2-\rho_1}{\rho_2+\rho_1}\right), \quad c_2^2 \sim \frac{g}{|k|}\left(\frac{\rho_3-\rho_2}{\rho_3+\rho_2}\right). \tag{7.37}$$

7.4. *Long-wave limit*

Passing to the long-wave limit $k \to 0$ gives

$$a_2 \to -g\frac{\rho_2(\rho_3-\rho_1)h_1h_b+\rho_3(\rho_2-\rho_1)h_1h_3+\rho_1(\rho_3-\rho_2)h_3h_b}{\rho_2\rho_3h_1+\rho_1\rho_2h_b+\rho_1\rho_3h_3}, \tag{7.38}$$

$$a_0 \to \frac{g^2(\rho_3-\rho_2)(\rho_2-\rho_1)h_1h_3h_b}{\rho_2\rho_3h_1+\rho_1\rho_2h_b+\rho_1\rho_3h_3}, \tag{7.39}$$

therefore we obtain the equation

$$\begin{aligned}&(\rho_2\rho_3h_1+\rho_1\rho_2h_b+\rho_1\rho_3h_3)c^4\\&-g[\rho_2(\rho_3-\rho_1)h_1h_b+\rho_3(\rho_2-\rho_1)h_1h_3+\rho_1(\rho_3-\rho_2)h_3h_b]c^2\\&+g^2(\rho_3-\rho_2)(\rho_2-\rho_1)h_1h_3h_b=0,\end{aligned} \tag{7.40}$$

which appeared also in de Melo Viríssimo & Milewski (2019) and Ratliff (2022), where it is obtained by other methods. We will prove in the following that (7.40) has four real roots for all values of the densities and all values of the (mean) depths h_1, h_3, h_b. To begin, we denote $c^2 = Z$ in (7.40) and obtain the second-degree equation in Z

$$\begin{aligned}&(\rho_2\rho_3h_1+\rho_1\rho_2h_b+\rho_1\rho_3h_3)Z^2\\&\quad-g[\rho_2(\rho_3-\rho_1)h_1h_b+\rho_3(\rho_2-\rho_1)h_1h_3+\rho_1(\rho_3-\rho_2)h_3h_b]Z\\&\quad+g^2(\rho_3-\rho_2)(\rho_2-\rho_1)h_1h_3h_b=0.\end{aligned} \tag{7.41}$$

Taking into account that $\rho_3 > \rho_2 > \rho_1$, and applying the Cauchy-Schwarz inequality, we have first

$$\begin{aligned}&\rho_2(\rho_3-\rho_1)h_1h_b+\rho_3(\rho_2-\rho_1)h_1h_3+\rho_1(\rho_3-\rho_2)h_3h_b\\&\geq 2h_1\sqrt{h_3h_b}\sqrt{\rho_2\rho_3(\rho_3-\rho_1)(\rho_2-\rho_1)}\\&+2h_b\sqrt{h_1h_3}\sqrt{\rho_1\rho_2(\rho_3-\rho_1)(\rho_3-\rho_2)}\\&+2h_3\sqrt{h_1h_b}\sqrt{\rho_1\rho_3(\rho_2-\rho_1)(\rho_3-\rho_2)}\\&>2\sqrt{(\rho_3-\rho_2)(\rho_2-\rho_1)}\left[\sqrt{\rho_2\rho_3}\,h_1\sqrt{h_3h_b}+\sqrt{\rho_1\rho_2}\,h_b\sqrt{h_1h_3}+\sqrt{\rho_1\rho_3}\,h_3\sqrt{h_1h_b}\right]\\&=2\sqrt{(\rho_3-\rho_2)(\rho_2-\rho_1)}\sqrt{h_1h_3h_b}\left[\sqrt{\rho_2\rho_3h_1}+\sqrt{\rho_1\rho_2h_b}+\sqrt{\rho_1\rho_3h_3}\right]\end{aligned}$$

https://doi.org/10.1017/jfm.2026.11138 Published online by Cambridge University Press

$$\geq 2\sqrt{(\rho_3-\rho_2)(\rho_2-\rho_1)}\sqrt{h_1h_3h_b}\sqrt{\rho_2\rho_3h_1+\rho_1\rho_2h_b+\rho_1\rho_3h_3}, \tag{7.42}$$

where for the last inequality we have used that ρ_i $(i=1,2,3)$, h_1, h_3, h_b are positive. By squaring in the obtained inequality, we see that the discriminant of (7.41) is strictly positive, i.e. (7.41) has two distinct real roots, which, by the Viète formulas, are positive. From the latter finding we infer that the fourth-order equation (7.40) has four real roots: two positive and two negative.

We obtain an approximation for the smaller root by neglecting c^4 in (7.40),

$$c_- := \pm\sqrt{\frac{g(\rho_3-\rho_2)(\rho_2-\rho_1)h_1h_3h_b}{\rho_2(\rho_3-\rho_1)h_1h_b+\rho_3(\rho_2-\rho_1)h_1h_3+\rho_1(\rho_3-\rho_2)h_3h_b}}, \tag{7.43}$$

which in turn is approximately equal to (5.33) when $\rho_1\approx\rho_2$ in the expression $\rho_1(\rho_3-\rho_2)h_3h_b\approx\rho_2(\rho_3-\rho_2)h_3h_b$.

By neglecting the last term in (7.40), we obtain an approximation for the larger root,

$$c_+ := \pm\sqrt{\frac{g[\rho_2(\rho_3-\rho_1)h_1h_b+\rho_3(\rho_2-\rho_1)h_1h_3+\rho_1(\rho_3-\rho_2)h_3h_b]}{\rho_2\rho_3h_1+\rho_1\rho_2h_b+\rho_1\rho_3h_3}}. \tag{7.44}$$

Under the further assumption that $\rho_1\approx\rho_2\approx\rho_3=\rho$ in the denominator and in the ratios ρ_i/ρ_j, we have

$$\begin{aligned} c_+ &\approx \pm\sqrt{\frac{g[\rho_2(\rho_3-\rho_1)h_1h_b+\rho_3(\rho_2-\rho_1)h_1h_3+\rho_1(\rho_3-\rho_2)h_3h_b]}{\rho^2(h_1+h_b+h_3)}} \\ &\approx \pm\sqrt{\frac{g}{h_1+h}\left(\frac{(\rho_2-\rho_1)h_1h_3}{\rho_2}+\frac{(\rho_3-\rho_2)h_3h_b}{\rho_3}+\frac{(\rho_3-\rho_1)h_1h_b}{\rho_3}\right)}, \end{aligned} \tag{7.45}$$

which is (5.33).

Therefore the approximation formulas for both models agree under the further assumption of small relative differences between densities, $|\rho_i-\rho_j|/\rho_n\ll 1$.

Finally, we point out that each propagation speed has its trace at every surface. For the largest propagation speed c_+ (mode 1), the ratio of the wave amplitudes η_2, η_3 of the upper and lower interfaces in the linear regime is $(\eta_2/\eta_3)_{c=c_+}>0$. In this case, both waves have the same polarity. For the slow-propagating mode c_- (mode 2), $(\eta_2/\eta_3)_{c=c_-}<0$, and in this case the waves have the opposite polarity. See e.g. the details in de Melo Viríssimo & Milewski (2019).

7.5. *Boussinesq regime for the rigid lid system*

The next example of evolution equations arising from (7.17), (7.20) and (7.21) is the Boussinesq regime. As a result, we obtain a coupled system of nonlinear evolution equations. We recall the expansions of the DN operators in the case under consideration (Craig *et al.* 2005; Ivanov *et al.* 2022):

$$G_1(\eta_2) = D\tanh(h_1D) - D\eta_2D + D\tanh(h_1D)\,\eta_2D\tanh(h_1D) + \cdots, \tag{7.46}$$

$$G(\eta_3) = D\tanh(h_bD) + D\eta_3D - D\tanh(h_bD)\,\eta_3D\tanh(h_bD) + \cdots, \tag{7.47}$$

$$\begin{aligned} \Gamma_{11}(\eta_2,\eta_3) = {} & D\coth(h_3D) + D\,\mathrm{csch}(h_3D)\,\eta_3D\,\mathrm{csch}(h_3D) \\ & + D\eta_2D - D\coth(h_3D)\,\eta_2D\coth(h_3D) + \cdots, \end{aligned} \tag{7.48}$$

$$\begin{aligned} \Gamma_{12}(\eta_2,\eta_3) = {} & -D\,\mathrm{csch}(h_3D) - D\,\mathrm{csch}(h_3D)\,\eta_3D\coth(h_3D) \\ & + D\coth(h_3D)\,\eta_2D\,\mathrm{csch}(h_3D) + \cdots, \end{aligned} \tag{7.49}$$

https://doi.org/10.1017/jfm.2026.11138 Published online by Cambridge University Press

$$\Gamma_{21}(\eta_2,\eta_3) = -D\,\mathrm{csch}(h_3D) - D\coth(h_3D)\,\eta_3 D\,\mathrm{csch}(h_3D) + D\,\mathrm{csch}(h_3D)\,\eta_2 D\coth(h_3D) + \cdots, \tag{7.50}$$

$$\Gamma_{22}(\eta_2,\eta_3) = D\coth(h_3D) + D\coth(h_3D)\,\eta_3 D\coth(h_3D) - D\eta_3 D - D\,\mathrm{csch}(h_3D)\,\eta_2 D\,\mathrm{csch}(h_3D) + \cdots. \tag{7.51}$$

We use these expansions in the Boussinesq regime, i.e. assuming that the small-amplitude parameters for each combination $\varepsilon_{ij} = |\eta_j|_{max}/h_i$ are of the same order of magnitude, say ε, for all i, j, and also that the long-wave parameters $\delta_j = 2\pi h_j/\lambda = kh_j$ are of the same order δ, and moreover $\varepsilon \ll 1$ and $\delta^2 \ll 1$ are of the same order as well. Furthermore, we recall the fact that the eigenvalue of D is the wavenumber k, so the action of D will generate a quantity of order δ. On the other hand, the multiplication by η_j will generate a quantity of order ε. Keeping this in mind, the relevant expansion of (7.12)–(7.15) in terms of the DN operators (7.46)–(7.51) is

$$A_{22} = A_{220}D^2 + A_{221}D^4 + B_{222}D\eta_2 D + B_{223}D\eta_3 D + \cdots, \tag{7.52}$$

$$A_{23} = A_{32} = A_{230}D^2 + A_{231}D^4 + B_{232}D\eta_2 D + B_{233}D\eta_3 D + \cdots, \tag{7.53}$$

$$A_{33} = A_{330}D^2 + A_{331}D^4 + B_{332}D\eta_2 D + B_{333}D\eta_3 D + \cdots, \tag{7.54}$$

where the expansion coefficients are

$$A_{220} = \frac{h_1(h_3\rho_3 + h_b\rho_2)}{h_1\rho_2\rho_3 + h_3\rho_1\rho_3 + h_b\rho_1\rho_2}, \tag{7.55}$$

$$A_{221} = -\frac{h_1^2\big(h_1h_3^2\rho_1\rho_3^2 + 2h_1h_3h_b\rho_1\rho_2\rho_3 + h_1h_b^2\rho_1\rho_2^2 + h_3^3\rho_2\rho_3^2 + 3h_3^2h_b\rho_2^2\rho_3 + 3h_3h_b^2\rho_2^3 + h_b^3\rho_2^2\rho_3\big)}{3(h_1\rho_2\rho_3 + h_3\rho_1\rho_3 + h_b\rho_1\rho_2)^2}, \tag{7.56}$$

$$B_{222} = \frac{-(h_3\rho_3 + h_b\rho_2)^2\rho_1 + h_1^2\rho_2\rho_3^2}{(h_1\rho_2\rho_3 + h_3\rho_1\rho_3 + h_b\rho_1\rho_2)^2}, \tag{7.57}$$

$$B_{223} = \frac{(\rho_2 - \rho_3)h_1^2\rho_2\rho_3}{(h_1\rho_2\rho_3 + h_3\rho_1\rho_3 + h_b\rho_1\rho_2)^2}, \tag{7.58}$$

$$A_{230} = \frac{h_1h_b\rho_2}{h_1\rho_2\rho_3 + h_3\rho_1\rho_3 + h_b\rho_1\rho_2}, \tag{7.59}$$

$$A_{231} = -\frac{h_1h_b\rho_2\big[6h_1h_bh_3\rho_2^2 + h_b(2h_1^2 + 3h_3^2)\rho_1\rho_2 + (3h_3^2 + 2h_b^2)h_1\rho_2\rho_3 + h_3(2h_1^2 + h_3^2 + 2h_b^2)\rho_1\rho_3\big]}{6(h_1\rho_2\rho_3 + h_3\rho_1\rho_3 + h_b\rho_1\rho_2)^2}, \tag{7.60}$$

$$B_{232} = -\frac{h_b\rho_1\rho_2[h_b\rho_2 + (h_1 + h_3)\rho_3]}{(h_1\rho_2\rho_3 + h_3\rho_1\rho_3 + h_b\rho_1\rho_2)^2}, \tag{7.61}$$

$$B_{233} = \frac{h_1\rho_3\rho_2[(h_3 + h_b)\rho_1 + h_1\rho_2]}{(h_1\rho_2\rho_3 + h_3\rho_1\rho_3 + h_b\rho_1\rho_2)^2}, \tag{7.62}$$

https://doi.org/10.1017/jfm.2026.11138 Published online by Cambridge University Press

$$A_{330} = \frac{h_b(h_1\rho_2 + h_3\rho_1)}{h_1\rho_2\rho_3 + h_3\rho_1\rho_3 + h_b\rho_1\rho_2} \tag{7.63}$$

$$A_{331} = -\frac{h_b^2\big(h_1^3\rho_1\rho_2^2 + 3h_1^2h_3\rho_2^3 + h_1^2h_b\rho_2^2\rho_3 + 3h_1h_3^2\rho_1\rho_2^2 + 2h_1h_3h_b\rho_1\rho_2\rho_3 + h_3^3\rho_1^2\rho_2 + h_3^2h_b\rho_1^2\rho_3\big)}{3(h_1\rho_2\rho_3 + h_3\rho_1\rho_3 + h_b\rho_1\rho_2)^2}, \tag{7.64}$$

$$B_{332} = \frac{h_b^2(\rho_1 - \rho_2)\rho_1\rho_2}{(h_1\rho_2\rho_3 + h_3\rho_1\rho_3 + h_b\rho_1\rho_2)^2}, \tag{7.65}$$

$$B_{333} = \frac{(h_1\rho_2 + h_3\rho_1)^2\rho_3 - h_b^2\rho_1^2\rho_2}{(h_1\rho_2\rho_3 + h_3\rho_1\rho_3 + h_b\rho_1\rho_2)^2}. \tag{7.66}$$

Since in the Boussinesq regime the equations are maximum quadratic in the field variables, (7.20) and (7.21) suggest that we need only the leading order of the quantities Φ_j^i and F_j:

$$\Phi_2^2 = \frac{h_1\rho_3\xi_2 - h_b\rho_1\xi_3}{h_1\rho_2\rho_3 + h_3\rho_1\rho_3 + h_b\rho_1\rho_2}, \tag{7.67}$$

$$\Phi_2^1 = -\frac{h_b\rho_2(\xi_2 + \xi_3) + h_3\rho_3\xi_2}{h_1\rho_2\rho_3 + h_3\rho_1\rho_3 + h_b\rho_1\rho_2}, \tag{7.68}$$

$$\Phi^3 = \frac{h_1(\xi_2 + \xi_3)\rho_2 + h_3\xi_3\rho_1}{h_1\rho_2\rho_3 + h_3\rho_1\rho_3 + h_b\rho_1\rho_2}, \tag{7.69}$$

$$\Phi_3^2 = \frac{h_1\rho_3\xi_2 - h_b\rho_1\xi_3}{h_1\rho_2\rho_3 + h_3\rho_1\rho_3 + h_b\rho_1\rho_2}. \tag{7.70}$$

Introducing the variables $\mathrm{u}_j = (\xi_j)_x$, we first notice that F_j in leading order are linear combinations of $\mathrm{u}_{j,x}$, while $\Phi_{j,x}^i$ are linear combinations of u_j only. However, we notice that $\mathcal{O}(h_j\mathrm{u}_{j,x}) = \mathcal{O}(kh_j\mathrm{u}_j) = \delta\,\mathcal{O}(\mathrm{u}_j) \ll \mathcal{O}(\mathrm{u}_j)$. Thus the terms with F_j in (7.20) and (7.21) can be neglected in comparison to the other terms with $\Phi_{j,x}^i$ (as in the water wave theory of a single layer). Then we obtain the system

$$\begin{aligned}
&\mathrm{u}_{2,t} + \frac{[\rho_2(h_1\rho_3\mathrm{u}_2 - h_b\rho_1\mathrm{u}_3)^2 - \rho_1(h_b\rho_2(\mathrm{u}_2 + \mathrm{u}_3) + h_3\rho_3\mathrm{u}_2)^2]_x}{2(h_1\rho_2\rho_3 + h_3\rho_1\rho_3 + h_b\rho_1\rho_2)^2} + (\rho_2 - \rho_1)g\eta_{2,x} = 0,\\
&\mathrm{u}_{3,t} + \frac{[\rho_3(h_1\rho_2(\mathrm{u}_2 + \mathrm{u}_3) + h_3\rho_1\mathrm{u}_3)^2 - \rho_2(h_1\rho_3\mathrm{u}_2 - h_b\rho_1\mathrm{u}_3)^2]_x}{2(h_1\rho_2\rho_3 + h_3\rho_1\rho_3 + h_b\rho_1\rho_2)^2} + (\rho_3 - \rho_2)g\eta_{3,x} = 0,\\
&\eta_{2,t} = -A_{220}\mathrm{u}_{2,x} + A_{221}\mathrm{u}_{2,xxx} - B_{222}[\eta_2\mathrm{u}_2]_x - B_{223}[\eta_3\mathrm{u}_2]_x\\
&\qquad - A_{230}\mathrm{u}_{3,x} + A_{231}\mathrm{u}_{3,xxx} - B_{232}[\eta_2\mathrm{u}_3]_x - B_{233}[\eta_3\mathrm{u}_3]_x,\\
&\eta_{3,t} = -A_{230}\mathrm{u}_{2,x} + A_{231}\mathrm{u}_{2,xxx} - B_{232}[\eta_2\mathrm{u}_2]_x - B_{233}[\eta_3\mathrm{u}_2]_x\\
&\qquad - A_{330}\mathrm{u}_{3,x} + A_{331}\mathrm{u}_{3,xxx} - B_{332}[\eta_2\mathrm{u}_3]_x - B_{333}[\eta_3\mathrm{u}_3]_x.
\end{aligned} \tag{7.71}$$

Letting $\rho_1 \to 0$, we obtain the two-layer domain with surface $y = \eta_2(x, t)$ and interface $y = \eta_3(x, t)$, whereby the coefficients A_{ijk}, B_{ijk} $(i, j \in \{1, 2\},\ k \in \{0, 1, 2, 3\})$ are

https://doi.org/10.1017/jfm.2026.11138 Published online by Cambridge University Press

given by

$$A_{220}=\frac{h_3\rho_3+h_b\rho_2}{\rho_2\rho_3},\quad A_{221}=-\frac{h_3^3\rho_3^2+3h_3^2h_b\rho_2\rho_3+3h_3h_b^2\rho_2^2+h_b^3\rho_2\rho_3}{3\rho_2\rho_3^2},$$
$$B_{222}=\frac{1}{\rho_2},\quad B_{223}=\frac{\rho_2-\rho_3}{\rho_2\rho_3},$$
$$A_{230}=\frac{h_b}{\rho_3},\quad A_{231}=-\frac{h_b\left[6h_bh_3\rho_2+\left(3h_3^2+2h_b^2\right)\rho_3\right]}{6\rho_3^2},\quad B_{232}=0,\quad B_{233}=\frac{1}{\rho_3},$$
$$A_{330}=\frac{h_b}{\rho_3},\quad A_{331}=-\frac{h_b^2(3h_3\rho_2+h_b\rho_3)}{3\rho_3^2},\quad B_{332}=0,\quad B_{333}=\frac{1}{\rho_3}. \tag{7.72}$$

Consequently, system (7.71) becomes

$$\begin{aligned}
&u_{2,t}+\frac{1}{\rho_2}u_2u_{2,x}+\rho_2g\eta_{2,x}=0,\\
&u_{3,t}+\frac{\rho_2-\rho_3}{\rho_2\rho_3}u_2u_{2,x}+\frac{1}{\rho_3}(u_2u_3)_x+\frac{1}{\rho_3}u_3u_{3,x}+(\rho_3-\rho_2)g\eta_{3,x}=0,\\
&\eta_{2,t}=-\frac{h_3\rho_3+h_b\rho_2}{\rho_2\rho_3}u_{2,x}-\frac{h_3^3\rho_3^2+3h_3^2h_b\rho_2\rho_3+3h_3h_b^2\rho_2^2+h_b^3\rho_2\rho_3}{3\rho_2\rho_3^2}u_{2,xxx}\\
&\qquad-\frac{1}{\rho_2}[\eta_2u_2]_x-\frac{\rho_2-\rho_3}{\rho_2\rho_3}[\eta_3u_2]_x\\
&\qquad-\frac{h_b}{\rho_3}u_{3,x}-\frac{h_b\left[6h_bh_3\rho_2+\left(3h_3^2+2h_b^2\right)\rho_3\right]}{6\rho_3^2}u_{3,xxx}-\frac{1}{\rho_3}[\eta_3u_3]_x,\\
&\eta_{3,t}=-\frac{h_b}{\rho_3}u_{2,x}-\frac{h_b\left[6h_bh_3\rho_2+\left(3h_3^2+2h_b^2\right)\rho_3\right]}{6\rho_3^2}u_{2,xxx}-\frac{1}{\rho_3}[\eta_3u_2]_x\\
&\qquad-\frac{h_b}{\rho_3}u_{3,x}-\frac{h_b^2(3h_3\rho_2+h_b\rho_3)}{3\rho_3^2}u_{3,xxx}-\frac{1}{\rho_3}[\eta_3u_3]_x,
\end{aligned} \tag{7.73}$$

which recovers the system obtained by Craig *et al.* (2005) on p. 1626, derived by employing similar methods involving expansions of the DN operators for two layers with a free surface.

The procedure utilised to obtain the Boussinesq system (7.73) highlights a general method for the derivation of nonlinear models for water waves propagation starting from the general system (7.17), (7.20) and (7.21).

7.6. *Limit to the full equations for two layers with a free surface*

The limit to the full equations for two layers with a free surface as they appear (however, in Hamiltonian form) in Craig *et al.* (2005) could be done by simply setting up $\rho_1=0$ in all formulas in this section. Furthermore, given a depth h^*, there is a relation between the DN operators $G_{ij}(h^*,\eta_l,\eta_u)$ and $\Gamma_{ij}(h^*,\eta_l,\eta_u)$, which reads

$$G_{11}(h^*,\eta_l,\eta_u)=\Gamma_{22}(h^*,\eta_l,\eta_u),\quad G_{12}(h^*,\eta_l,\eta_u)=\Gamma_{21}(h^*,\eta_l,\eta_u), \tag{7.74}$$
$$G_{21}(h^*,\eta_l,\eta_u)=\Gamma_{12}(h^*,\eta_l,\eta_u),\quad G_{22}(h^*,\eta_l,\eta_u)=\Gamma_{11}(h^*,\eta_l,\eta_u), \tag{7.75}$$

where $y=\eta_l(x,t)$ is the lower boundary of the domain, and $y=\eta_u(x,t)$ is the upper boundary of the domain.

https://doi.org/10.1017/jfm.2026.11138 Published online by Cambridge University Press

From (7.6), we obtain

$$\xi_2 := \rho_2(\varphi_2)_{s_2}, \quad \xi_3 := \rho_3(\varphi_3)_{s_3} - \rho_2(\varphi_2)_{s_3}. \tag{7.76}$$

We define the operator (essentially the operator B in Craig *et al.* (2005) for the free surface case.)

$$\mathcal{B} := \rho_3\Gamma_{22} + \rho_2 G, \tag{7.77}$$

which is self-adjoint. Then we have

$$B^{-1} = \frac{1}{\rho_2} G_1^{-1}\Gamma_{12}\mathcal{B}^{-1}, \quad (B^{-1})^* = \frac{1}{\rho_2}\mathcal{B}^{-1}\Gamma_{21}G_1^{-1}. \tag{7.78}$$

From (7.7) and (7.8), we obtain

$$(\varphi_2)_{s_2} = \frac{1}{\rho_2}\xi_2 =: \Phi_2^2(\xi_2), \tag{7.79}$$

$$(\varphi_2)_{s_3} = -\mathcal{B}^{-1}\left[G\xi_3 + \frac{\rho_3}{\rho_2}\Gamma_{21}\xi_2\right] =: \Phi_3^2(\eta_i, \xi_i). \tag{7.80}$$

Then from (7.5), (7.79) and (7.80) after some calculations, we have

$$(\varphi_3)_{s_3} = -G^{-1}[\Gamma_{21}(\varphi_2)_{s_2} + \Gamma_{22}(\varphi_2)_{s_3}] = \mathcal{B}^{-1}\left[-\Gamma_{21}\xi_2 + \Gamma_{22}\xi_3\right] =: \Phi^3(\eta_i, \xi_i). \tag{7.81}$$

In view of (7.74)–(7.75), these formulas reproduce (2.26)–(2.28) of Craig *et al.* (2005). Next, from (7.12)–(7.15), we obtain the expressions for the operators:

$$A_{22} = \frac{1}{\rho_2}\Gamma_{11} - \frac{\rho_3}{\rho_2}\Gamma_{12}\mathcal{B}^{-1}\Gamma_{21}, \tag{7.82}$$

$$A_{23} = -\Gamma_{12}\mathcal{B}^{-1}G, \tag{7.83}$$

$$A_{32} = \frac{1}{\rho_2}\left(-\mathcal{B} + \rho_3\Gamma_{22}\right)\mathcal{B}^{-1}\Gamma_{21} = -G\mathcal{B}^{-1}\Gamma_{21} = A_{23}^*, \tag{7.84}$$

$$A_{33} = \Gamma_{22}\mathcal{B}^{-1}G. \tag{7.85}$$

The operator A_{33} is self-adjoint since G and Γ_{22} are self-adjoint operators (Craig *et al.* 2005). Indeed, we can write it formally as

$$A_{33} = \frac{1}{\rho_3}\Gamma_{22}\left(1 + \frac{\rho_2}{\rho_3}\Gamma_{22}^{-1}G\right)^{-1}\Gamma_{22}^{-1}G. \tag{7.86}$$

In the leading order, $(\rho_2/\rho_3)\,|\Gamma_{22}^{-1}G| = (\rho_2/\rho_3)\,|\tanh(kh_b)\tanh(kh_3)| < 1$, so, at least in some domain for the values of (k, η_2, η_3) in the neighbourhood of $(0, 0, 0)$, we have an expansion

$$A_{33} = \frac{1}{\rho_3}\left(G - \frac{\rho_2}{\rho_3}G\Gamma_{22}^{-1}G + \frac{\rho_2^2}{\rho_3^2}G\Gamma_{22}^{-1}G\Gamma_{22}^{-1}G + \cdots\right), \tag{7.87}$$

from which it is evident that $A_{33} = A_{33}^*$, thus $A_{33} = G\mathcal{B}^{-1}\Gamma_{22}$. The operator A_{22} is also self-adjoint since Γ_{11} is self adjoint and $\Gamma_{12}^* = \Gamma_{21}$; cf. Craig *et al.* (2005).

https://doi.org/10.1017/jfm.2026.11138 Published online by Cambridge University Press

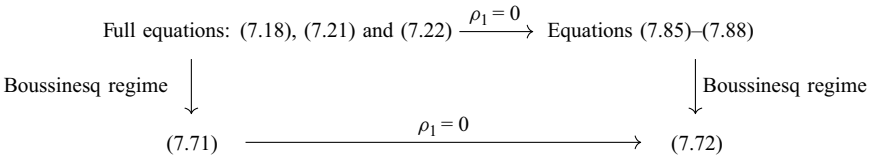


Figure 2. Relations between the derived models: limits and approximations.

The functionals F_2 and F_3 are as in (7.16); then the full equations of motion are the same as in (7.17), (7.20) and (7.21) (with $\rho_1 = 0$), i.e. explicitly,

$$\eta_{2,t} = \left(\frac{1}{\rho_2}\Gamma_{11} - \frac{\rho_3}{\rho_2}\Gamma_{12}\mathcal{B}^{-1}\Gamma_{21}\right)\xi_2 - \Gamma_{12}\mathcal{B}^{-1}G\xi_3 =: F_2(\eta_i, \xi_i), \tag{7.88}$$

$$\eta_{3,t} = G\mathcal{B}^{-1}[-\Gamma_{21}\xi_2 + \Gamma_{22}\xi_3] =: F_3(\eta_i, \xi_i), \tag{7.89}$$

$$\xi_{2,t} = -\frac{\rho_2(\Phi^2_{2,x})^2 - 2F_2\xi_{2,x}\eta_{2,x} - \rho_2 F_2^2}{2(1+\eta^2_{2,x})} - \rho_2 g\eta_2, \tag{7.90}$$

$$\xi_{3,t} = -\frac{\rho_3(\Phi^3_x)^2 - \rho_2(\Phi^2_{3,x})^2 - 2F_3\xi_{3,x}\eta_{3,x} + (\rho_2-\rho_3)F_3^2}{2(1+\eta^2_{3,x})} - (\rho_3-\rho_2)g\eta_3. \tag{7.91}$$

Equation (7.88) follows also from (7.4), (7.79) and (7.80); and (7.89) follows from (7.5) and (7.81). The DN operators depend on η_2 and η_3 in a complicated nonlinear way; however, as we have mentioned, there is a systematic approach for their derivation. In the Boussinesq limit, the above system produces the system (7.73) (see the derivation in Craig *et al.* 2005), although we have obtained it as a limit from (7.71). Figure 2 shows the relations between the derived models in this section.

8. Conclusions and outlook

We have presented a Hamiltonian formulation for the nonlinear governing equations describing irrotational two-dimensional inviscid and incompressible water flows with piecewise constant density stratification in a three-layer fluid with a flat bottom, a free surface and two interfaces. We then introduced in each layer Dirichlet–Neumann (DN) operators with the help of which we re-expressed the Hamiltonian of the system and the equations of motion for the free surface and for the interfaces. The Hamiltonian formulation and the leading-order DN operators have allowed us to obtain linearised equations for small-amplitude waves at the surface and interfaces. We derived a bi-cubic equation representing the dispersion relation, in the short- and long-wave limits, we have analysed the solutions of this equation, and we obtained approximate expressions for the speed of the left- and right-running waves on the surface and at the internal interfaces.

The results presented here open new avenues of investigations, of which we mention a few.

(i) Formulas (3.30), (3.35) and (3.36) give (through the Hamiltonian variables) the boundary values of the velocity potential that extends analytically to the interior of the fluid body. This will lead to in-depth investigations of important properties of the flow pertaining to the pressure, velocity field and particle trajectories; cf. e.g. Henry & Villari (2022).

(ii) Since the three-layer scenario renders the inclusion of a current with piecewise linear profile more realistic and natural (as e.g. in Constantin *et al.* 2016; Constantin &

https://doi.org/10.1017/jfm.2026.11138 Published online by Cambridge University Press

Ivanov 2019), various results from the two-layer case concerning wave–current interactions in stratified flows are amenable to further extensions. In particular, the presence of currents in the layers will allow the formation of Kelvin–Helmholtz instabilities at the interfaces (see e.g. Benjamin & Bridges 1997*a*,*b*). In this case, the instability condition at each interface will incorporate the current components in the three layers, thereforedisplaying an increased level of complexity to the problem that will require the pursuit of significant new research in this direction.

(iii) Furthermore, a detailed study of the DN operators will lead to weakly nonlinear models for various propagation regimes that will be deduced from the equations presented in their general form; cf. (3.42), (3.43), (3.44), (3.53), (3.54), (3.55) in the case of a free surface, and (7.17), (7.20), (7.21) in the case of a flat surface. An example was given by the derivation of the coupled system (7.73) in the Boussinesq regime. From the weakly nonlinear regimes such as the Korteweg–de Vries regime, the soliton dynamics can be recovered, which is of practical importance given the fact that the solitons are stable and easier to observe in comparison to other wave types. The central role in the derivation of such systems is played by the DN operators and their expansions. Our motivation was based on the understanding that in the present research environment, the use of symbolic computation will increase dramatically (perhaps powered by AI), and the expansions of the DN operators should be highly facilitated.

The utilisation of the Hamiltonian formulation and the DN operators allows a concise derivation of model equations for this type of stratified flow. We have demonstrated how these equations can be written in an explicit final form for all scales and propagation regimes. If necessary, the expansions of the DN operators lead to particular equations for a specific (small) scale parameter (up to the desired order of the small parameter). For many configurations, especially the most common ones, these expansions are already known, which solves the problem immediately. Highlighting the significance of the DN operators, we point out that recent years have seen a surge in the study of both the full nonlinear water wave problem and various approximate nonlinear water wave models. This progress is driven by a combination of methods focusing on DN operators and Hamiltonian systems – cf. Baldi *et al.* (2018), Berti, Franzoi & Maspero (2021), Bona, Lannes & Saut (2008), Constantin & Ivanov (2019), Clamond (2022), Lannes (2005), Alvarez-Samaniego & Lannes (2008), Andrade & Nachbin (2018), Ivanov *et al.* (2022) – as well as methods for numerical computation of quantities, expressed by DN operators in Guyenne & Părău (2016), Guyenne (2017) and Canning Gregory & Nicholls (2012), following the pioneering work of Craig & Sulem (1993).

Acknowledgements. The authors thank three anonymous reviewers and the editor (Prof. J. Kirby) for insightful comments and suggestions that significantly improved the paper.

Funding. R.I. gratefully acknowledges financial support from Research Ireland under grant no. 21/FFP-A/9150. C.I.M. acknowledges support from the project "Nonlinear studies of stratified oceanic and atmospheric flows", funded by the European Union–NextGenerationEU and the Romanian Government under the National Recovery and Resilience Plan for Romania, contract no. 760040/23.05.2023, cod PNRR-C9-I8-CF 185/22.11.2022, through the Romanian Ministry of Research, Innovation and Digitalization, within Component 9, Investment I8.

Declaration of interests. On behalf of all authors, the corresponding author states that there is no conflict of interest.

Data availability statement. The reported results are of a purely theoretical nature, and no data have been used supporting these results.

https://doi.org/10.1017/jfm.2026.11138 Published online by Cambridge University Press

References

Alvarez-Samaniego, B. & Lannes, D. 2008 Large time existence for 3D water-waves and asymptotics. *Invent. Math.* **171**, 485–541.

Andrade, D. & Nachbin, A. 2018 A three-dimensional Dirichlet-to-Neumann operator for water waves over topography. *J. Fluid Mech.* **845**, 321–345.

Baines, P.G. 1995 *Topographic Effects in Stratified Flows*, Cambridge Monographs in Mathematics. Cambridge University Press.

Baldi, P., Berti, M., Haus, E. & Montalto, R. 2018 Time quasi-periodic gravity water waves in finite depth. *Invent. Math.* **214**, 739–911.

Benton, G.S. 1954 The occurrence of critical flow and hydraulic jumps in a multi-layer fluid system. *J. Meteorol.* **11**, 139–150.

Berti, M., Franzoi, L. & Maspero, A. 2021 Traveling quasi-periodic water waves with constant vorticity. *Arch. Rat. Mech. Anal.* **240**, 99–202.

Benjamin, T.B. & Bridges, T.J. 1997*a* Reappraisal of the Kelvin–Helmholtz problem. I. Hamiltonian structure. *J. Fluid Mech.* **333**, 301–325.

Benjamin, T.B. & Bridges, T.J. 1997*b* Reappraisal of the Kelvin–Helmholtz problem. II. Interaction of the Kelvin–Helmholtz, superharmonic and Benjamin–Feir instabilities. *J. Fluid Mech.* **333**, 327–373.

Bona, J.L., Lannes, D. & Saut, J.-C. 2008 Asymptotic models for internal waves. *J. Mathématiques Pures Appliquées* **89**, 538–566.

Camassa, R., Falqui, G., Ortenzi, G., Pedroni, M. & Ho, T.T.V. 2021 Hamiltonian aspects of three-layer stratified fluids. *J. Nonlinear Sci.* **31**, 70.

Canning Gregory, R. & Nicholls, D.P. 2012 Numerical simulation of a weakly nonlinear model for internal waves. *Commun. Comput. Phys.* **12**, 1461–1481.

Choi, W. & Camassa, R. 1996 Weakly nonlinear internal waves in a two-fluid system. *J. Fluid Mech.* **313**, 83–103.

Choi, W. & Camassa, R. 1999 Fully nonlinear internal waves in a two-fluid system. *J. Fluid Mech.* **396**, 1–36.

Clamond, D. 2022 Explicit Dirichlet–Neumann operator for water waves. *J. Fluid Mech.* **950**, A33.

Compelli, A. & Ivanov, R. 2017 The dynamics of flat surface internal geophysical waves with currents. *J. Math. Fluid Mech.* **19**, 329–344.

Compelli, A., Ivanov, R. & Todorov, M. 2018 Hamiltonian models for the propagation of irrotational surface gravity waves over a variable bottom. *Phil. Trans. R. Soc. Lond. A* **376**, 20170091.

Compelli, A., Ivanov, R., Martin, C. & Todorov, M. 2019 Surface waves over currents and uneven bottom. *Deep-Sea Res. II* **160**, 25–31.

Constantin, A. 2013 Some three-dimensional nonlinear equatorial flows. *J. Phys. Oceanogr.* **43**, 165–175.

Constantin, A. 2014 Some nonlinear, equatorially trapped, nonhydrostatic internal geophysical waves. *J. Phys. Oceanogr.* **44**, 781–789.

Constantin, A. & Ivanov, R.I. 2019 Equatorial wave–current interactions. *Commun. Math. Phys.* **370**, 1–48.

Constantin, A., Ivanov, R.I. & Martin, C.-I. 2016 Hamiltonian formulation for wave–current interactions in stratified rotational flows. *Arch. Rat. Mech. Anal.* **221**, 1417–1447.

Constantin, A., Ivanov, R. & Prodanov, E. 2007 Nearly-Hamiltonian structure for water waves with constant vorticity. *J. Math. Fluid Mech.* **9**, 1–14.

Constantin, A. & Johnson, R.S. 2015 The dynamics of waves interacting with the equatorial undercurrent. *Geophys. Astrophys. Fluid Dyn.* **109**, 311–358.

Constantin, A. & Johnson, R.S. 2017 A nonlinear, three-dimensional model for ocean flows, motivated by some observations of the Pacific Equatorial Undercurrent and thermocline. *Phys. Fluids* **29**, 056604.

Cotter, C.J., Holm, D.D. & Percival, J.R. 2010 The square root depth wave equations. *Proc. R. Soc. Lond. A* **466**, 3621–3633.

Craig, W., Guyenne, P. & Kalisch, H. 2005 Hamiltonian long wave expansions for free surfaces and interfaces. *Commun. Pure Appl. Maths* **58**, 1587–1641.

Craig, W., Guyenne, P., Nicholls, D.P. & Sulem, C. 2005 Hamiltonian long-wave expansions for water waves over a rough bottom. *Proc. R. Soc. Lond. A* **461**, 839–873.

Craig, W., Guyenne, P. & Sulem, C. 2011 Coupling between surface and internal waves. *Nat. Hazards* **57**, 617–642.

Craig, W., Guyenne, P. & Sulem, C. 2012 The surface signature of internal waves. *J. Fluid Mech.* **710**, 277–303.

Craig, W., Guyenne, P. & Sulem, C. 2015 Internal waves coupled to surface gravity waves in three dimensions. *Commun. Math. Sci.* **13** (4), 893–910.

https://doi.org/10.1017/jfm.2026.11138 Published online by Cambridge University Press

CRAIG, W. & SULEM, C. 1993 Numerical simulation of gravity waves. *J. Comput. Phys.* **108**, 73–83.
CUSHMAN-ROISIN, B. & BECKERS, J.-M. 2011 *Introduction to Geophysical Fluid Dynamics: Physical and Numerical Aspects*. Academic Press.
ESCHER, J., KNOPF, P., LIENSTROMBERG, C. & MATIOC, B.-V. 2020 Stratified periodic water waves with singular density gradients. *Annali Matematica Pura Applicata* **199**, 1923–1959.
EVANS, L.C. 2010 *Partial Differential Equations*, Graduate Studies in Mathematics. AMS.
FEDOROV, A.V. & BROWN, J.N. 2009 Equatorial waves. In *Encyclopedia of Ocean Sciences* (ed. J. Steele), pp. 3679–3695. Academic Press.
GILL, A. 1982 *Atmosphere–Ocean Dynamics*. Academic Press.
GREENHILL, A.G. 1886 Wave motion in hydrodynamics. *Am. J. Maths* **9** (1), 62–96.
GRIMSHAW, R., GUO, C., HELFRICH, K. & VLASENKO, V. 2014 Combined effect of rotation and topography on shoaling oceanic internal solitary waves. *J. Phys. Oceanogr.* **44**, 1116–1132.
GUYENNE, P. 2017 A high-order spectral method for nonlinear water waves in the presence of a linear shear current. *Comput. Fluids* **154**, 224–235.
GUYENNE, P. & PĂRĂU, E. 2016 An operator expansion method for computing nonlinear surface waves on a ferrofluid jet. *J. Comput. Phys.* **321**, 414–434.
HENRY, D. & VILLARI, G. 2022 Flow underlying coupled surface and internal waves. *J. Differ. Equ.* **310**, 404–442.
HUTTULA, T. 2012 Stratification in lakes. In *Encyclopedia of Lakes and Reservoirs* (ed. L. Bengtsson, R.W. Herschy & R.W. Fairbridge), Encyclopedia of Earth Sciences Series. Springer.
IVANOV, R.I. & MARTIN, C.I. Hamiltonian approach to three-layer flows with currents. in preparation.
IVANOV, R.I., MARTIN, C.I. & TODOROV, M.D. 2022 Hamiltonian approach to modelling interfacial internal waves over variable bottom. *Phys. D: Nonlinear Phenom.* **433**, 133190.
KAKUTANI, T. & YAMASAKI, N. 1978 Solitary waves in a two-layer fluid. *J. Phys. Soc. Japan* **45**, 674–679.
KESSLER, W.S. & MCPHADEN, M.J. 1995 Oceanic equatorial waves and the 1991–93 El Niño. *J. Clim.* **8**, 1757–1774.
KODAIRA, T., WASEDA, T., MIYATA, M. & CHOI, W. 2016 Internal solitary waves in a two-fluid system with a free surface. *J. Fluid Mech.* **804**, 201–223.
LAMB, H. 1932 *Hydrodynamics*, 6th edn. Cambridge University Press.
LANNES, D. 2005 Well-posedness of the water-waves equations. *J. Am. Math. Soc.* **18** (3), 605–654.
MARSHALL, J. & PLUMB, R.A. 2016 *Atmosphere, Ocean and Climate Dynamics: An Introductory Text*. Academic Press.
MARTIN, C.I. 2021 Azimuthal equatorial flows in spherical coordinates with discontinuous stratification. *Phys. Fluids* **33**, 026602.
MASSEL, S. 2015 *Internal Gravity Waves in the Shallow Seas*. Springer International Publishing.
MATIOC, A.-V. 2012 Steady internal water waves with a critical layer bounded by the wave surface. *J. Nonlinear Math. Phys.* **19**, 1250008.
DE MELO VIRÍSSIMO, F. & MILEWSKI, P.A. 2019 Three-layer flows in the shallow water limit. *Stud. Appl. Maths* **142**, 487–512.
OLVER, P.J. 1993 *Applications of Lie Groups to Differential Equations*. Springer-Verlag.
OSTROVSKY, L.A. & HELFRICH, K.R. 2019 Some new aspects of the joint effect of rotation and topography on internal solitary waves. *J. Phys. Oceanogr.* **49**, 1639–1649.
OVSYANNIKOV, L.V. 1979 Two-layer 'shallow water' model. *J. Appl. Mech. Tech. Phys.* **20**, 127–135.
PRODANOV, E. 2022*a* Isolation intervals of the real roots of the parametric cubic equation and improved complete root classification. *Adv. Theory Simul.* **5**, 2100638.
PRODANOV, E. 2022*b* The Siebeck–Marden–Northshield theorem and the real roots of the symbolic cubic equation. *Results Maths* **77**, 126.
RATLIFF, D.J. 2022 Genuine nonlinearity and its connection to the modified Korteweg–de Vries equation in phase dynamics. *Nonlinearity* **35**, 30–65.
REED, M. & SIMON, B. 1975 *Fourier Analysis*, *Self-Adjointness*. New York: Academic Press. (Methods of Modern Mathematical Physics, vol. II)
SHINTANI, T. & UMEYAMA, M. 2001 Response of a three-layer stratified water body in wind flume. In *3rd International Symposium on Environmental Hydraulics, Tempe, Arizona, USA*.
SIMMONS, H., CHANG, M.-H., CHANG, Y.-T., CHAO, S.-Y., FRINGER, O., JACKSON, C.R. & KO, D.S. 2011 Modeling and prediction of internal waves in the South China Sea. *Oceanography* **24**, 88–99.
SUTHERLAND, B.R. 2010 *Internal Gravity Waves*. Cambridge University Press.
VALLIS, G. 2017 *Atmospheric and Oceanic Fluid Dynamics: Fundamentals and Large-Scale Circulation*. Cambridge University Press.

https://doi.org/10.1017/jfm.2026.11138 Published online by Cambridge University Press

WAHLÉN, E. 2007 A Hamiltonian formulation of water waves with constant vorticity. *Lett. Math. Phys.* **79**, 303–315.
WAHLÉN, E. 2008 Hamiltonian long-wave approximations of water waves with constant vorticity. *Phys. Lett. A* **372**, 2597–2602.
WHITHAM, G.B. 1999 *Linear and Nonlinear Waves*. Wiley.
YIH, C.-S. 1980 *Stratified Flows*. Academic Press.
ZAKHAROV, V.E. 1968 Stability of periodic waves of finite amplitude on the surface of a deep fluid. *J. Appl. Mech. Tech. Phys.* **9**, 86–89.
https://oceanexplorer.noaa.gov/technology/ctd/ctd.html.
https://www.bodc.ac.uk/data/bodc_database/ctd/.
https://podaac.jpl.nasa.gov/dataset/OMG_L2_CTD).

https://doi.org/10.1017/jfm.2026.11138 Published online by Cambridge University Press